Copolymerization studies of ethylene and trimethylsilyl protected 1-alkenols using a

Brookhart-type α-diimine nickel(II) dibromide precatalyst

by

Heidi K. Murray

A thesis submitted to the Department of Chemistry

in conformity with the requirements for

the degree of Master of Science

Queen's University

Kingston, Ontario, Canada

January, 2009

Abstract

There has been considerable interest over the past decade in the preparation and applications of copolymers of ethylene with functionalized polar olefins. Such copolymers are expected to exhibit a variety of potentially very useful properties such as paintability, adhesion to polar surfaces, and miscibility with polar polymers such as polyesters and polyamides, but there are limitations associated with producing copolymers of ethylene with polar monomers via Ziegler-Natta processes. Many classes of Ziegler-Natta catalysts, especially those of the early transition metals (Ti and Zr), are highly oxophilic and hence are poisoned by functionalities such as -OH groups. This problem can in principle be alleviated by implementing the use of protecting groups such as $-OSiMe_3$, which has previously been shown to be an effective masking agent both for steric reasons and because O-Si π bonding decreases the Lewis basicity of the ether oxygen atom. One can also utilize late transition metal catalyst systems, which are generally less Lewis acidic and therefore less susceptible to poisoning by functional groups.

In this thesis the results of an investigation of the copolymerization of ethylene with $CH_2=CH(CH_2)_nOSiMe_3$ (n = 1, 2, 8) will be presented. We have been using MAO activated dibromo[1,4-bis(2,6-diisopropylphenyl)acenaphthenediimine]nickel(II) **(D)** as catalyst, as this system is known to produce reasonably linear polyethylene and hence may be expected to produce essentially LLDPE containing $-(CH_2)_nOSiMe_3$ branches. The latter can be hydrolyzed to give polar $-(CH_2)_nOH$ branches.

Acknowledgements

I would like to begin by thanking Dr. Michael Baird for the opportunity to work in his lab. He has been a wonderful mentor and a source of guidance. The lab has become my second home. I would also like to thank Dr. Guojun Liu, Dr. Ralph Whitney and Dr. S. Parent for all their advice and support.

The Baird group has become my new family. I would like to thank Dr. Goran Stojcevic, Dr. Emily Mitchell and Dr. John Brownie for being wonderful resources throughout my research. I would like to thank the present members of the Baird group, Danielle Norton, Shalyn Littlefield, Kevin Fowler, Andrew Frazer and Gregory Vettese for making the lab fun. I would also like to thank Dr. David Edwards for his assistance with my DSC analyses.

Finally, I would like to thank my parents and siblings for their continual support throughout the course of my studies. Their unconditional love has truly provided me with the strength and determination needed to succeed.

Table of Contents   **Page**

Chapter 1 – Introduction

List of Tables **Page**

List of Figures Page

List of Abbreviations and Symbols

Ar	argon
atm	atmospheres
d	doublet
dd	doublet of doublet
ddt	doublet of doublet of triplet
ºC	degrees Celsius
Et	ethyl group
GPC	gel permeation chromatography
η	hapticity
h	hour
HDPE	high density polyethylene
^{i}Pr	isopropyl group
IR	infrared spectroscopy
J	coupling constant
kg	kilogram
L	litre
LDPE	low density polyethylene
LLDPE	linear low density polyethylene
m	multiplet
m	meta
mg	milligram
min	minutes

mL	milliliter
mol	moles
mol %	mole percent
MAO	methylaluminoxane
Me	methyl
MHz	megahertz
M_n	number average molecular weight
M_w	weight average molecular weight
NMR	nuclear magnetic resonance
o	ortho
p	para
PE	polyethylene
PDI	polydispersity index
Ph	phenyl
ppm	parts per million
q	quartet
r.t	room temperature
R	alkyl group
s	singlet
t	triplet
T_g	glass transition temperature
T_m	melting temperature
$TCE\text{-}d_2$	1,1,2,2-tetrachloroethane

TMS   trimethylsilane

Chapter 1.   Introduction

1.0.0   Polyethylene

There is a significant demand for polyolefins, especially polyethylene due to the numerous applications in industry and everyday life and especially the use of the end products in bulk.[1-4a] Polyethylene is used in a variety of applications such as in coatings, house wares and packaging films. This has fueled the transformation of the polyethylene industry into a fast growing, multibillion dollar per annum industry.[5,6] The three major classes of polyethylene (Figure 1-1) are HDPE (high density polyethylene) (**i**), LLDPE (linear low density polyethylene) (**ii**) and LDPE (low density polyethylene) (**iii**).

(i) HDPE

(ii) LLDPE

(iii) LDPE
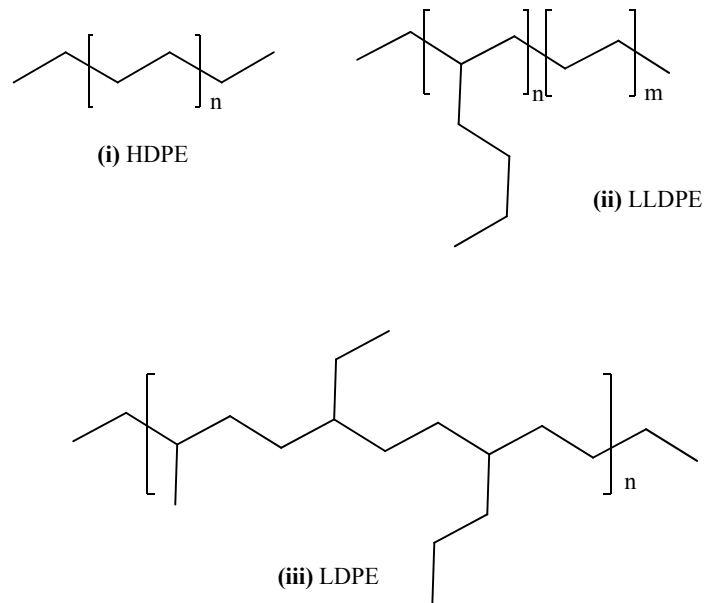
Figure 1-1: Three classes of polyethylene (PE)

High density polyethylene is a linear (no or few branches) and highly crystalline homopolymer of ethylene. HDPE has a high melting temperature ($T_m \approx 130$ °C) and is usually prepared by the Ziegler-Natta polymerization process. Low density polyethylene

1

is a branched (branches of varied length such as methyl, ethyl, etc.) homopolymer of ethylene prepared under high temperature and pressure conditions via a free-radical process.[7] LLDPE (random branches of identical length) on the other hand, is a random copolymer of ethylene with α-olefins such as 1-hexene. LLDPE is produced using metallocene and Ziegler-Natta based coordination techniques. This random incorporation of branches disrupts the crystalline packing, thus lowering the melting temperature.

1.0.1 Polymer Molecular Weight Analysis

The polymer's physical properties (tensile strength, toughness, heat resistance) are directly related to the molecular weight of the polymer sample.[4b] During synthetic polymerization processes, termination of the growing chains occurs at different stages, producing polymer chains of varied lengths. The processability of a polymer is affected by the degree of branching within the polymer backbone and in part by the molecular weight, therefore limiting its application. The two average molecular weights most used are the number averaged molecular weight (M_n) and the weight average molecular weight (M_w).

M_n is the arithmetic mean of the total weight of the molecules present in the polymer sample divided by the total number of molecules. This is shown in equation 1-1, below, where N_i is the number of moles of polymer chains which have molecular weight M_i. M_n is usually determined by gel permeation chromatography (GPC).[4b]

$$M_n = \Sigma N_i M_i / \Sigma N_i \qquad \textbf{eq. 1-1}$$

M_w is obtained by dividing the sum of the squares of the molecular weights by the sum of the molecular weights of all the polymer chains in the sample. This number (M_w) is always larger than M_n, except in monodispersed systems (when $M_n = M_w$) and it is usually determined by GPC.[4b] The ratio of M_w/M_n provides the polydispersity index (PDI) of the polymer mixture. Equations 1-2 and 1-3 show the M_w and PDI respectively.

$$M_w = \Sigma N_i M_i{}^2 / \Sigma N_i M_i \qquad \textbf{eq. 1-2}$$

$$PDI = M_w / M_n \qquad \textbf{eq. 1-3}$$

1.1.0   Ziegler-Natta Polymerization Mechanism

Pioneering work was done by Ziegler and Natta in developing catalytic systems which polymerize ethylene and propylene under mild reaction conditions (1 atm, 25 °C).[8,9] The homopolymers produced were highly linear, having few branches in contrast to the LDPE produced under radical processes as mentioned above. For their work they received a Nobel Prize in chemistry (1963). The accepted mechanism is known as the Cossee-Arlman mechanism.[10a,b] Figure 2-1 shows the general polymerization mechanism for these heterogeneous catalytic systems.
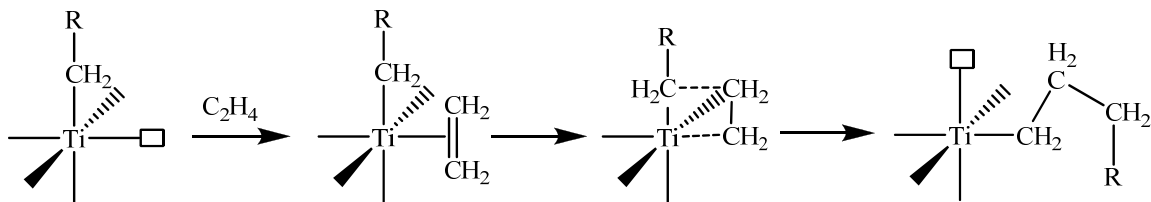
Figure 2-1: Ziegler-Natta mechanism of polymerization

1.1.1   Initiation and Propagation

TiCl$_3$ is activated by the cocatalyst AlR$_3$ (R is an alkyl group) which alkylates the metal and provides a vacant site *cis* to the alkyl ligand upon abstraction of a chloride ligand from the catalytic precursor TiCl$_3$. Olefin coordination occurs at the vacant site which upon insertion into the alkyl metal bond forms a four membered transition state. Another monomer can be subsequently coordinated and inserted at the accessible metal-centered vacant site. The active site is metal-centered and subsequent chain growth occurs there. Figure 2-2 shows the initiation and propagation processes.
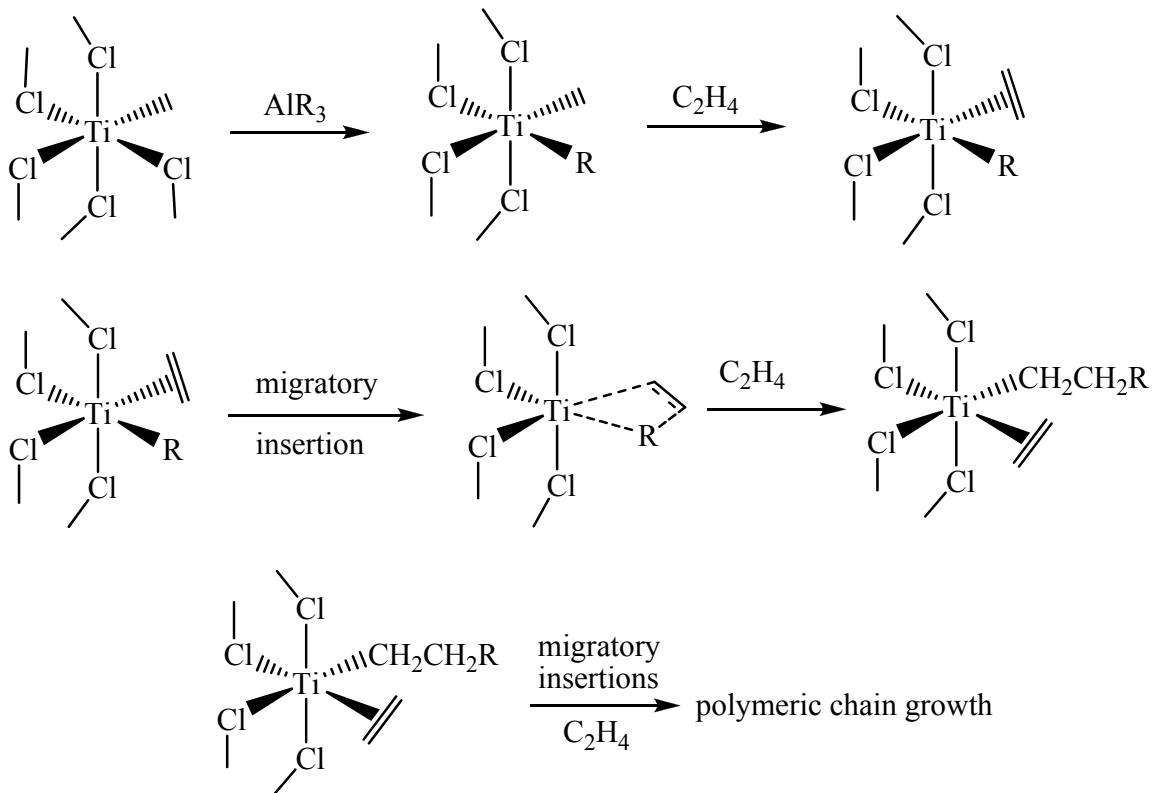
Figure 2-2: Ziegler-Natta initiation and propagation mechanism

Despite the numerous applications of polyolefins, there are limitations to their uses. These hydrocarbon polymers are hydrophobic, lacking polar functional groups. This lack has introduced various problems affiliated with the compatibility, adhesive and

paintability properties of polyolefins.[11,12] In the late 1980's polymer chemists thus envisioned the importance and impact that the incorporation of polar functionalities into hydrocarbon polymer chains might have. The random incorporation of functionalized monomers would alter the mechanical and chemical properties of these polymers, thus widening their potential applications. As a result there has been considerable interest in the syntheses of new, functionalized polymers. Relevant studies will be discussed herein.

The principal problem associated with the homo- and copolymerization of polar monomers with early metal (e.g. Ti, Zr) catalytic systems is catalyst poisoning (deactivation). The polar functionality preferentially binds to the oxophilic metal center, thus preventing monomer coordination and insertion (Figure 2-3). In contrast, late metal (e.g. Ni, Pd) catalytic systems are less Lewis acidic and are therefore more tolerant to polar functionalities, allowing olefin coordination and subsequent insertion.
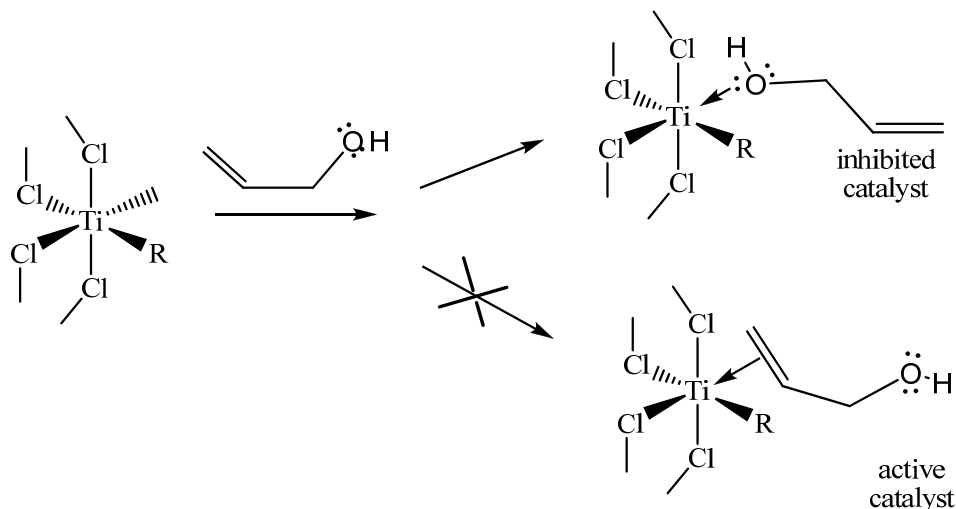
Figure 2-3: Pathway for early metal catalyst (TiCl₃) 'poisoning' by polar monomer addition

1.1.2 Late Transition Metal Olefin Polymerization and Chain Walking

The polyethylene produced by late transition metal systems is different from those produced by the early metals (d^0 catalysts). The polymer backbone has random branches and branches upon branches of varied lengths.[4c] The mechanism by which this occurs is shown in Figure 2-4 below.
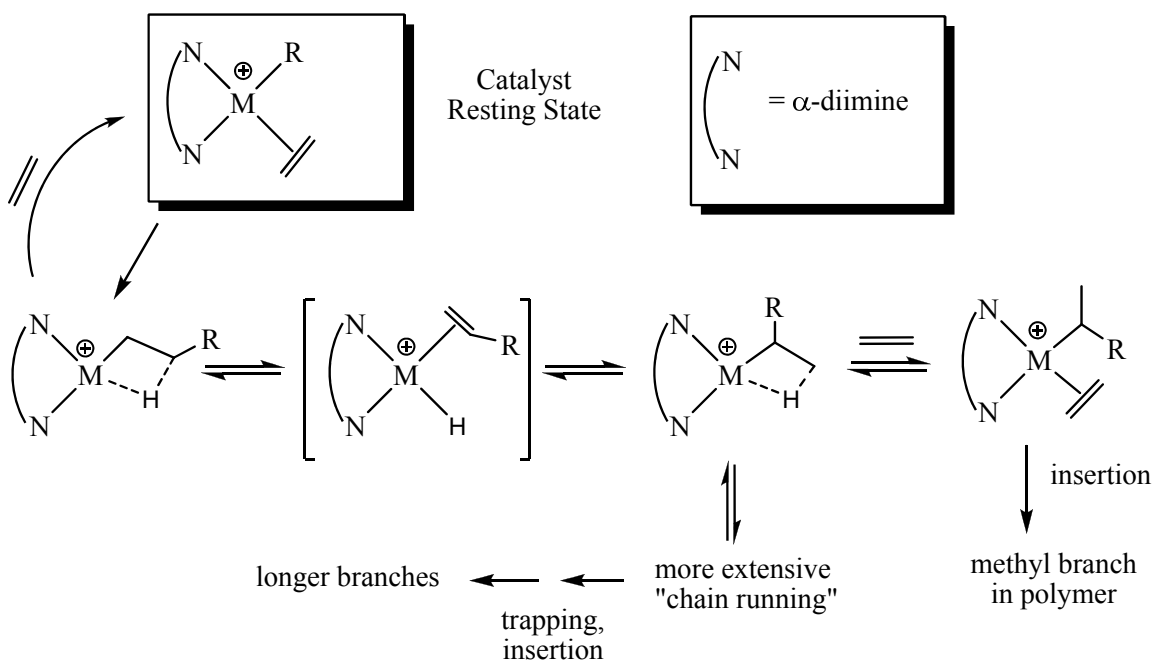
Figure 2-4: Late transition metal (Ni, Pd) mechanism for polymerization of ethylene

Branched polyethylene is normally produced with d^8 metal systems because of chain-walking processes. Chain-walking occurs when the metal centre of the β-agostic alkyl species migrates along the polymer backbone by a series of β-hydride elimination and reinsertion reactions.[4c]

6

1.2.0   Literature review

For the scope of this thesis focus was placed on the advances made with respect to the development of functionalized comonomers and the subsequent copolymerization with ethylene, propylene and/or other α-olefins. The main focus will be on direct copolymerization processes. The main protecting groups investigated within the literature will be presented below.

1.2.1   Siloxy Protecting Groups

Sivak and Cullo in 1988 investigated and patented the Ziegler-Natta polymerization of siloxy group (-OSiR$_3$ where R = aryl, alkyl, etc… groups) containing alkenes in the preparation of polymers containing functional groups.[13] For example H$_2$C=CH(CH$_2$)$_4$OSiMe$_3$ was prepared using 5-hexen-1-ol and SiMe$_3$Cl and was copolymerized with propene in the presence of a Ziegler-Natta catalyst. Upon removal of the silyl groups by hydrolysis, the functionalized copolymer was obtained as is shown in Figures 2-5 and 2-6. The adhesive and dyeability properties were investigated and are discussed below. Previously the use of Ziegler- Natta catalysts to copolymerize monomers containing functional groups had not been developed.

$$CH_2=CH(CH_2)_nOH \quad + \quad ClSiR_3 \quad \longrightarrow \quad CH_2=CH(CH_2)_nOSiR_3 \quad + \quad HCl \uparrow$$

$$n = 3\text{-}10$$
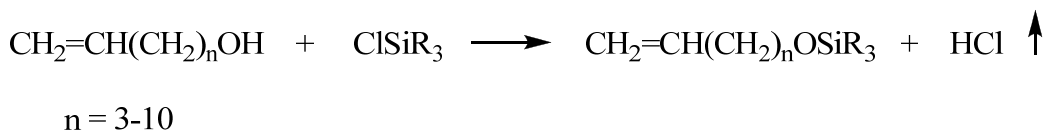
Figure 2-5: Pathway for siloxy functional monomer syntheses

$$CH_2{=}CHCH_3 \ + \ CH_2{=}CH(CH_2)_nOSiR_3 \longrightarrow \ ...YYY\overset{|}{Y}YYY...\!\!\underset{(CH_2)_nOSiR_3}{}$$

$$...YYY\overset{|}{Y}YYY...\!\!\underset{(CH_2)_nOSiR_3}{} \ + \ H_2O \longrightarrow \ ...YYY\overset{|}{Y}YYY...\!\!\underset{(CH_2)_nOH}{} \ + \ HOSiR_3$$

$$Y = \ \left[-CH_2-\underset{CH_3}{\overset{|}{CH}}- \right] \ \text{and} \ V = \ \left[-CH_2-\overset{|}{CH}\!- \right]$$

Figure 2-6: Pathway for copolymerization of siloxy functionalized comonomers with propene

To samples of the above mentioned copolymer and the propylene homopolymer, a dye (rhodamine, n-butanol and water) solution was added and the mixtures were refluxed for 4 h. The resulting precipitates were filtered, treated with a mixture of water/n-butanol and detergent, and vacuum dried. The resulting copolymer was coloured pink to a greater extent than the homopolymer. This was attributed to the incorporated 5-hexen-1-ol (5 mol %).

To investigate the differences in the adhesive properties between the copolymer and homopolymer, the following test was done. A sample of the copolymer was placed between two pieces of aluminum foil and then placed between the heated (193 ºC) platens of a hydraulic press. After being pressurized to 30,000 psig for a few minutes and then cooled to room temperature, the aluminum foil could not be removed mechanically from the copolymer film. The foil had to be digested using a caustic solution. In contrast, the homopolymer was pressure treated in an identical manner and, on completion the foil was easily removed mechanically leaving the polymer film intact. These results provided evidence of the potential impact these copolymers may have on the polyolefin industry.

1.2.2 Alkylboron Protecting Groups

In the late 1980's to early 1990's, Chung and coworkers investigated the use of organoboranes as a template in the synthesis of functionalized monomers and for subsequent homo- and copolymerization studies via a Ziegler- Natta process.[12] Initially a series of polyalcohols was synthesized using borane monomers as intermediates. The borane functionalized α-olefins were obtained by the monohydroboration of the appropriate diene with a dialkylborane such as 9-borabicyclo[3.3.1]nonane (9-BBN) (Figure 2-7). Due to the stability of the alkenylborane monomers to the titanium- and aluminum-based Ziegler-Natta catalyst, they were readily homopolymerized. The resulting polyboranes were then transformed into a variety of functionalities (polyalcohols or polyacids) via $NaOH/H_2O_2$ oxidation. The general homopolymerization pathway is shown in Figure 2-7.
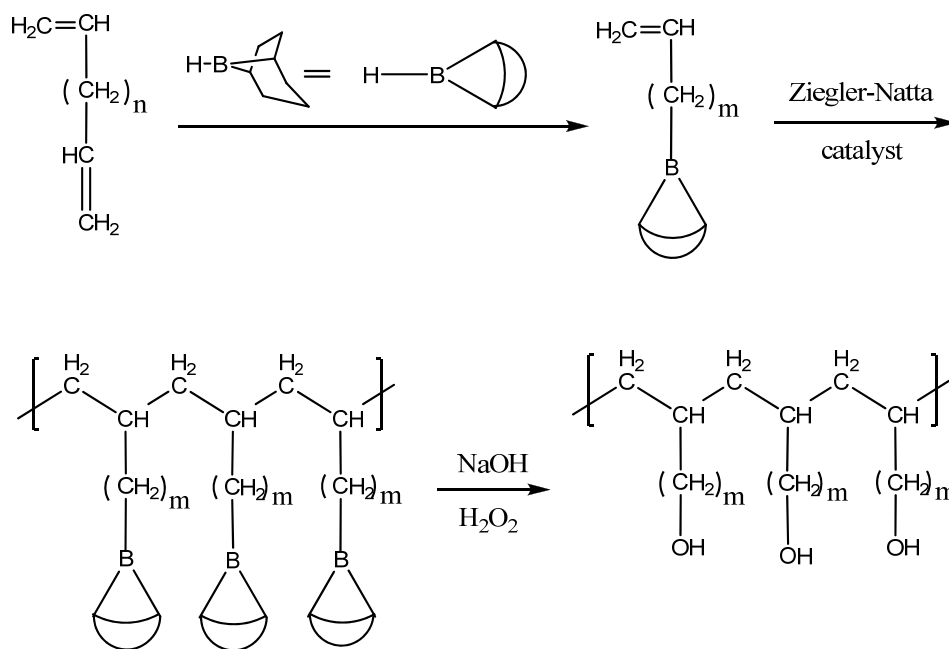
where n > / = 1 and m = n + 2

Figure 2-7: General synthetic pathway for homopolymerization of polyalcohols via boron protected intermediates

The syntheses of the polyborane and polyalcohol were further confirmed by ^{11}B-NMR, IR and TGA analyses. Based on the thermogravimetric analyses in an inert atmosphere (e.g. Ar), the polyalcohols exhibited high thermal stabilities, exhibiting <3 % weight loss at 300 ºC and decomposing only above 400 ºC. This thermal stability is significantly different from poly(vinyl) alcohol which dehydrates at 170 ºC and decomposes at 250 ºC.[14] The stability is attributed to the spacing between the hydroxyl group and the polymer backbone. The DSC exhibited a glass transition temperature (T_g) and a melting temperature (T_m) of 57 ºC and 110 ºC respectively. This is attributed to the partial crystallinity of the polyalcohol due to strong intermolecular interactions resulting from hydrogen bonding.

Based on those preliminary results, the copolymerization of 5-hexenyl-9-BBN and 1-octene was then investigated.[15] The copolymer formed was subsequently oxidized to produce poly(octene-*co*-hexenol), and the resulting copolymers were characterized by IR and NMR spectroscopy, GPC and DSC analyses. The percentage of hexenol varied from 0 to 100 %.

After successfully investigating the importance and use of borane-containing polyolefins in the development of functionalized homo- and copolymers,[12,15] Chung *et al*. later went on to study the copolymerization of α-olefins with borane protected monomers using metallocene catalysts **(A)** and **(B)** (Figure 3-1).[16] Here the goal was to get high degrees of incorporation of the borane containing α-olefins which, upon oxidation via NaOH/H_2O_2 treatment, would provide hydroxyl end groups. The copolymerization of ethylene and 5-hexenyl-9-BBN was studied using precatalysts Cp_2ZrCl_2 **(A)** and $Et(Ind)_2ZrCl_2$ **(B)**, using MAO as the co-catalyst (Figure 3-1). It was found that the best incorporation (up to 2.30 mol %) of the borane monomer was obtained with the $Et(Ind)_2ZrCl_2$/MAO system. The catalyst activity increased as the amount of borane monomer used was increased, which was not anticipated. The Cp_2ZrCl_2/MAO system yielded a lower incorporation of the borane monomer (1.22 mol %) under similar conditions (> 5000 equiv. MAO, 30 ºC). In contrast, when the heterogeneous Ziegler-Natta catalyst ($TiCl_3$/$AlEt_2Cl$) was used, no incorporation of the borane monomer was observed, thus providing evidence for the potential of metallocene-based systems to copolymerize functionalized α-olefins.

(A)   **(B)**
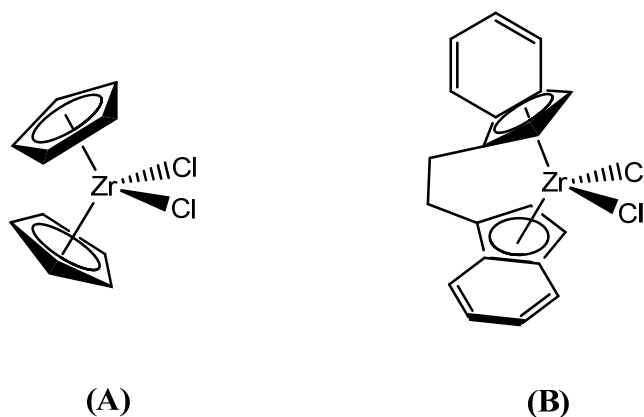
Figure 3-1: Zirconocene-based precatalysts

1.3   Early Metal Metallocene Catalysts for Polymerization Studies

In an effort to develop versatile functionalized copolymers via direct copolymerization, a large number of publications reported research into the use of metallocene based catalysts, such as **(A)** and **(B)**, during the 1990s.[17-23] The potential advantages of metallocene catalysts over traditional Ziegler-Natta heterogeneous catalysts include the following.

1. The catalytic systems are homogenous; therefore all active sites are in principle accessible to all molecules in solution, thus increasing the activity. The activity as a result is often 100 times greater than those of conventional Ziegler- Natta type catalysts.

2. Polyolefins with narrow molecular weight distributions ($M_w/M_n \approx 2$) are often obtained due to the "single-site" nature of the catalysts.

3. These catalytic systems can provide stereochemical control over the polymer microstructure.

4. Polyolefins can be produced with regularly distributed, long- and/or short-chained branches along the polymer chain. This allows for the development of different materials due to the ability to change their mechanical properties or create new ones. This will then lead to new applications.

The overall polymerization mechanism of metallocene-based catalysts is shown in Figure 3-2, using zirconocene dichloride as the precatalyst and methylaluminoxane (MAO) as co-catalyst.
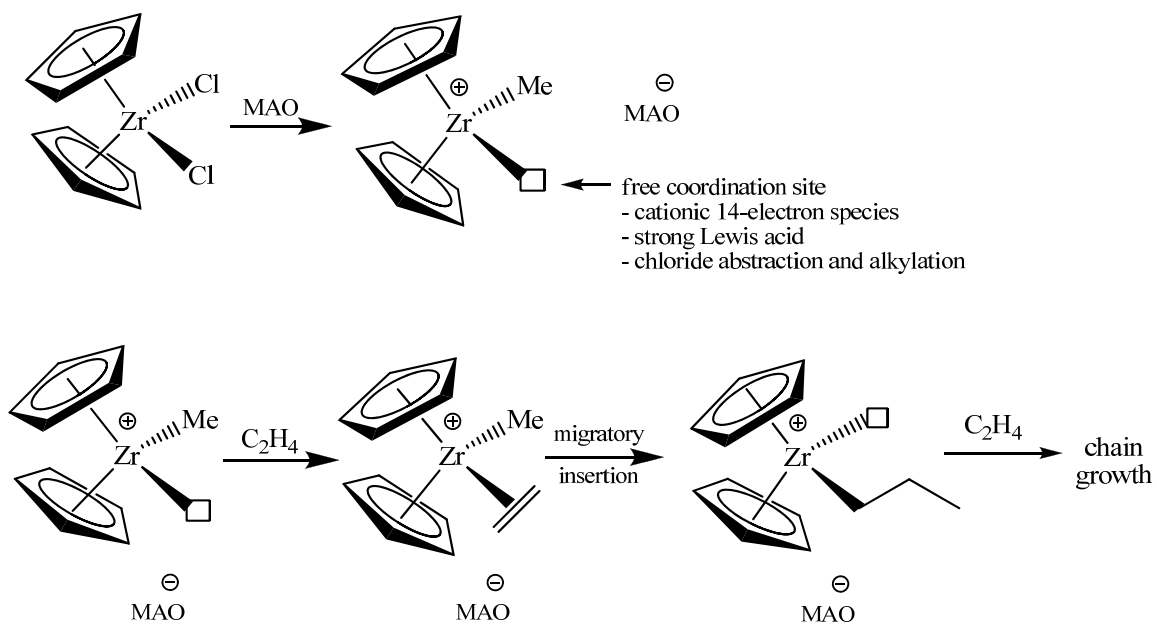
Figure 3-2: Metallocene-based mechanism of olefin polymerization with zirconocene dichloride

1.4 Activation of Coordination Precatalysts

1.4.1 Methylaluminoxane (MAO) as co-catalyst

Methylaluminoxane, discovered by Sinn and Kaminsky, is formed by the controlled hydrolysis of trimethylaluminum, and while its stoichiometry approximates $-[Al(CH_3)O]_n-$, its exact structure is unknown. The possible structures are shown in Figure 4-1.[24a,b,c]

(a) linear

(c) cyclic

(b) caged
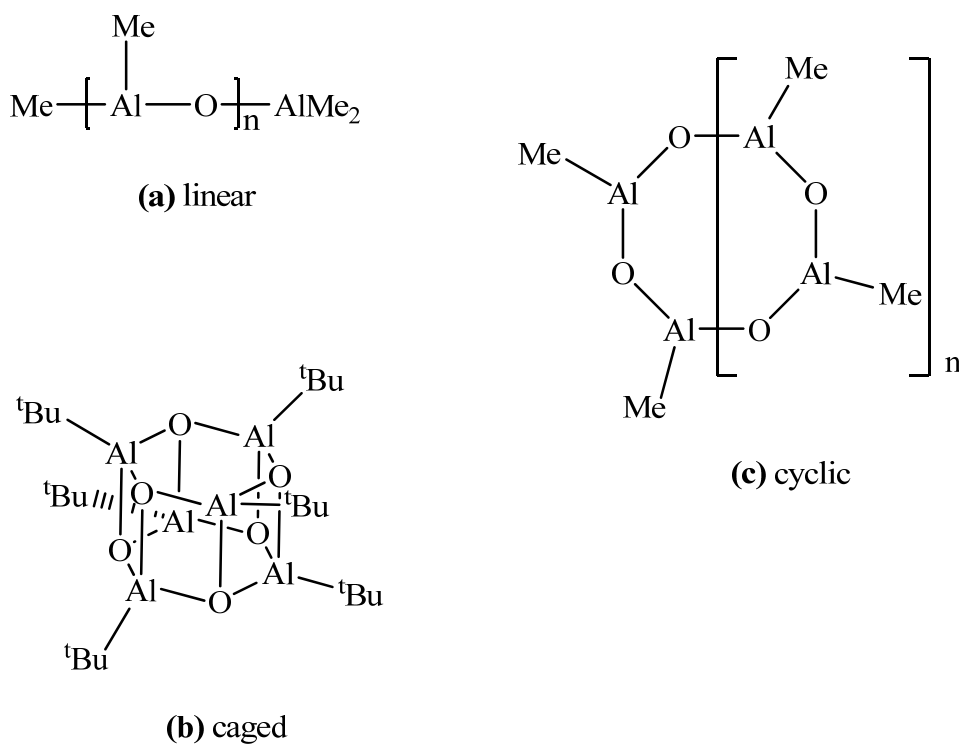
Figure 4-1: Possible structures of methylaluminoxane (MAO)

MAO is an effective activator for metallocene (group 4 transition metals) precatalysts,[25] activation occurring through halogen abstraction followed by methylation (Figure 3-2).

1.5   Late Metal Catalytic Systems for Polymerization Studies

In an effort to develop a catalytic system that incorporates the high activities of the early transition metals and the greater functional group tolerance of the late transition metals, Brookhart and co-workers have investigated nickel catalysts of the type shown in Figure 5-1.[26] The use of these systems, particularly for the homo- and copolymerization of ethylene with α-olefins and polar comonomers, is of particular interest to this group. The catalysts are based on the bulky, sterically-hindered, neutral chelating α-diimine ligands shown,[26] and have been found to be active for the homopolymerization of ethylene and its copolymerization with polar comonomers (acrylates) and α-olefins when activated appropriately.

$X = Cl, Br$

$R = H, Me,$

$R' = {}^iPr, Me, etc.$

Activator $= MAO$

(C)
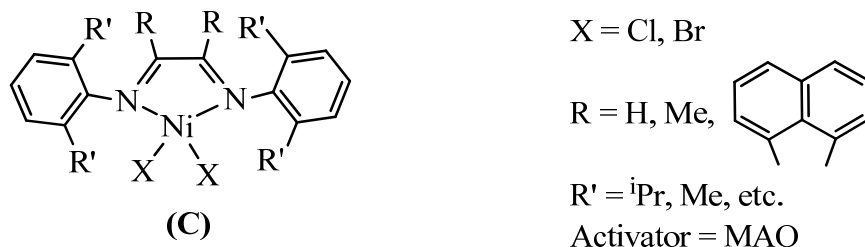
Figure 5-1: Brookhart's aryl-substituted nickel(II) α-diimine complexes

Brookhart's group discovered that ortho-substituted aryl α-diimine nickel(II) catalysts generally produce high molecular weight, branched polyethylene (LLDPE).[7] The α-diimine ligands **(C)** are synthesized via the Lewis or Bronsted acid catalyzed condensation of α,β-diketones with two equivalents of an alkyl- or arylamine. The simplest catalytic precursors are the neutral nickel(II) dihalides. The simplest pathway to the dibromide precursors involves the addition of the appropriate ligands to

dibromodimethoxyethanenickel(II) ((dme)NiBr$_2$) (Figure 5-2). This reaction involves the displacement of the labile dimethoxyethane ligand. The catalyst is generated by the *in situ* activation by methylaluminoxane.[26]
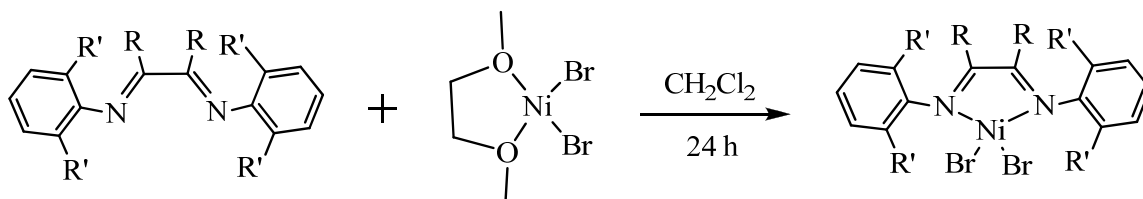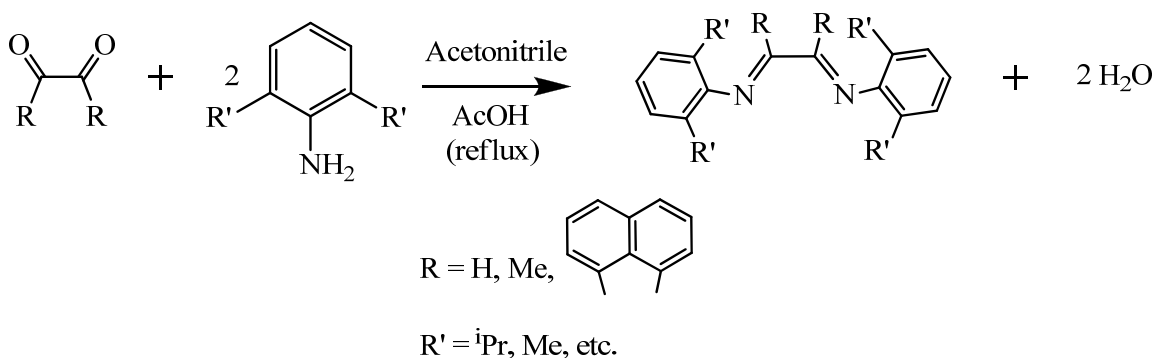
Figure 5-2: General synthetic pathway to nickel(II) dibromide catalyst precursors

1.5.1 Effects of modifying the structure and polymerization conditions on branched polyethylene produced by nickel(II) dihalide catalyst precursors

The mechanism by which branched polyethylene is produced is shown below in Figure 5-3.[7,4c] The mechanism by which chain walking occurs with nickel(II) systems was explained in Section 1.1.2. Chain propagation occurs via monomer (ethylene) coordination followed by a series of migratory insertions.
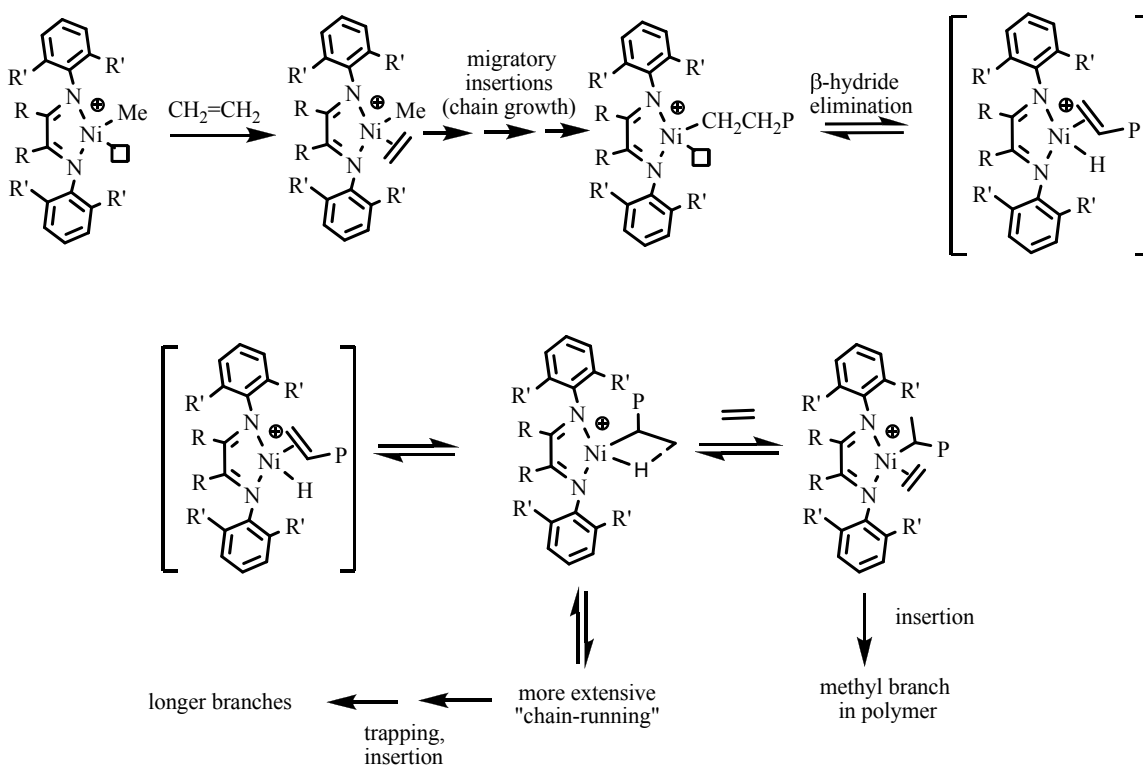
Figure 5-3: The mechanism of chain propagation, branching and chain running (□ = vacant site; P – polymeryl ligand)

Branches of variable lengths are produced along the chain by β-hydride elimination reactions followed by reinsertion at the β-carbon. After the reinsertion, ethylene can coordinate at the vacant site and chain propagation can continue. The degree of branching can be determined by comparing the relative ratios of the CH, CH_3 and CH_2 peak

17

integrations obtained from the ^{1}H-NMR spectrum of the polymer. The degree of branching within the polymer is determined by the lifetime of the cationic alkyl species (Figure 5-3).

The degree of branching is increased as the steric bulk of R' in the ligand increases.[7] This bulky R' hinders the coordination of the incoming monomer, inhibiting (slowing) the rate of chain propagation. This inhibition thus results in a greater occurrence of chain walking (Section 1.1.2), resulting in a more highly branched polymer.

The degree of branching decreases as the ethylene pressure is increased (increased ethylene concentration).[7] Catalyst activity and molecular weight are largely unaffected. The lifetime of the cationic alkyl complex is decreased and, as a result, the occurrence of β-hydride elimination is lowered, preventing reinsertion at the β-carbon and subsequent chain running.

Polymer branching is increased while the melting temperatures (T_m) and molecular weights are decreased as the temperature is increased.[7] The overall reaction kinetics are affected by varying the reaction temperature. Therefore it is possible to compensate for increased reaction pressures by increasing the temperature in order to maintain the same degree of branching within the polymer.

1.6   Research aim of this thesis

The objective of this thesis is to utilize Brookhart's α-diimine nickel(II) precatalyst **(D)** (Figure 6-1) system to investigate the copolymerization of ethylene with olefinic silyl ethers $(CH_2=CH(CH_2)_nOSiMe_3...n = 1, 2, 8)$.[26a] It is anticipated that copolymers of ethylene with such monomers would resemble LLDPE and that hydrolysis of the siloxy groups would then yield LLDPE with branches containing OH end groups, materials which could be very interesting.
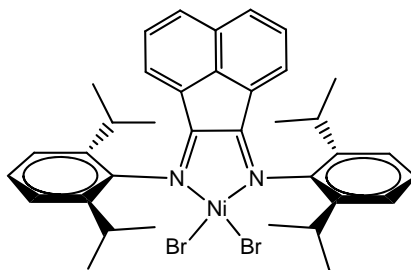
(D)

Figure 6-1: Dibromo[1,4-bis(2,6-diisopropylphenyl)acenaphthenediimine]nickel(II)

This precatalyst system was chosen as the polyethylene obtained by Brookhart *et al.* reported relatively high T_m of 122 ºC and low number of branches 71 per 1000 C. As expected, less branching was obtained when the pressure was increased to 4 atm.[26a]

Therefore, the goal of this thesis is to vary the polymerization conditions (temperature, comonomer equivalents, etc.) to obtain high degrees of polar comonomer incorporation into the polyethylene backbone. The relationship between the length of the spacer group between the polar functionality and the C=C double bond of the comonomers on the degree of incorporation will also be investigated. The results obtained should provide further insight into the factors which influence the degree of incorporation of polar functionalities into polyolefins.

Chapter 2.   Experimental

2.1.0   Chemical Supplies

All research chemicals used were purchased from Sigma Aldrich, unless stated otherwise, and were used without further purification. All deuterated (NMR) solvents were purchased from Cambridge Isotope Laboratories Inc. The NMR solvents were dried and degassed according to the procedures outlined in the physical and analytical methods section 2.1.1.

2.1.0.1 Homo- and Copolymerization Studies and Polar Monomer Syntheses

Cp_2ZrMe_2 were synthesized as in the literature[27] and stored at -30 ºC in a glovebox freezer. Lithium perchlorate (95 % Sigma Aldrich), 9-decen-1-ol (98 % Alfa Aesar), 3-buten-1-ol (96 % Sigma Aldrich), allyl alcohol (99 + % Sigma Aldrich) and 1,1,1,3,3,3-hexamethyldisilazane (HMDS, 97 % Sigma Aldrich) were used as received. Polymerization grade ethylene (Grade 3.0) was purchased from Praxair and was dried prior to use by passage through a column of activated 4 Å molecular sieves. The sieves were dried under reduced pressure while being heated for 24 h and then cooled to room temperature before purging with ethylene for approximately 30 min prior to use. Methylaluminoxane (10 wt % in toluene) was purchased from Sigma Aldrich and stored in a refrigerator (3 ºC) before being used under inert (argon) conditions.

2.1.1 Physical and Analytical Methods

All experiments were carried out under inert conditions using purified argon and standard Schlenk line techniques or an Mbraun Labmaster glovebox. Deoxygenated solvents, toluene, ethyl ether, hexanes, methylene chloride (CH_2Cl_2) and tetrahydrofuran (THF) were purchased and dried by passing through activated alumina columns. The water content (ppm) present in each solvent was determined by Karl-Fischer titrations. Based on these results, further drying was done for THF, CH_2Cl_2 and ethyl ether by storing each solvent over activated 4 Å molecular sieves (pellets). Benzene-d_6 and methylene chloride-d_2 were dried over calcium hydride (CaH_2), vacuum distilled and stored over activated 4 Å molecular sieves (pellets) in the glovebox. Deuterated chloroform ($CDCl_3$) was stored over activated 4 Å molecular sieves (pellets). 1,1,2,2-tetrachloroethane-d_2 (TCE-d_2) and chlorobenzene-d_5 (C_6D_5Cl) were used as received.

^{1}H-NMR spectra were run on Bruker AV300, 400, 500 or 600 spectrometers. All chemical shifts were referenced to TMS. All samples were prepared in 5 mm diameter tubes with approximately 0.6 mL of the selected deuterated solvent. Samples in CD_2Cl_2, $CDCl_3$, benzene-d_6 or toluene-d_8 were done at ambient temperature (r.t.). High temperature ^{1}H-NMR spectra were obtained at 120 ºC on the Bruker AV400 using TCE-d_2 as the solvent.

IR analyses were done on a Perkin Elmer Spectrum One FT-IR spectrometer at a spectral resolution of 4 cm^{-1}. Samples were prepared by dissolving the homo and copolymers in chlorobenzene for at least twenty-four hours followed by smearing the resulting solutions unto a sodium chloride (NaCl) disk. The slow evaporation of the solvent from the surface of the disk was done prior to analysis.

Differential scanning calorimetry (DSC) was done using a Perkin Elmer DSC 7 (TAC 7/DX). Polymer samples (~ 5 mg) were placed in aluminum pans and a ramping rate of 5.00 ºC/min was used, starting at 30 ºC and ramping up to 140 ºC. Three cycles were done for each sample, and the data from the second cycle were used for analysis.

2.2.0   Synthesis of [N'N-(2,6-Diisopropylphenyl)imino]acenaphthene
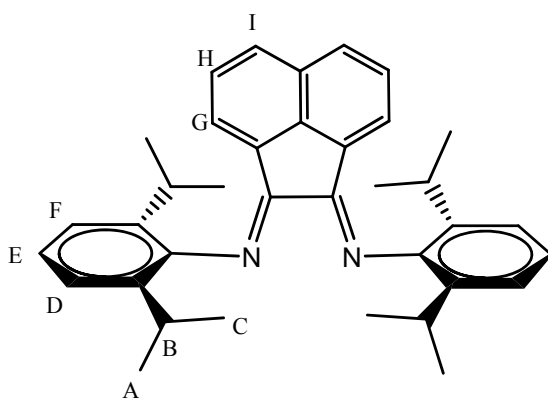
This ligand was synthesized following the literature procedure.[28] A solution of acenaphthenequinone (technical grade, 4.040g, 22.2 mmol) in 195 mL of acetonitrile was heated (~80 ºC) for 30 min, and then 36 mL of glacial acetic acid was added and heating was continued until the acenaphthenequinone completely dissolved. 10 mL (48 mmol) of 2,6-diisopropylaniline was added to the hot solution, which was refluxed for another 1.5 h. The solution was cooled to room temperature and the yellow precipitate of [N-(2,6-diisopropylphenyl)imino]acenaphthene was filtered, washed with hexanes and air-dried. Yield: 7.609 g, 69 %. ^{1}H-NMR (Section 3.1.0.1, Figure 7-2) (CDCl$_3$, 300 MHz, 25 ºC): δ 0.98 (d, 12H **(A)**, ^3J = 6.91 Hz), 1.25 (d, 12H **(C)**, ^3J = 6.66 Hz), 3.05 (sept, 4H **(B)**), 6.65 (d, 2H **(G)**, ^3J = 6.91 Hz), 7.28 (m (overlapping peaks), 6H **(D)**, **(E)**, **(F)**), 7.38 (t,

2H **(H)**), 7.89 (d, 2H **(I)**, ^3J = 8.19 Hz). The ^{1}H-NMR (CDCl$_3$, 300 MHz, 24 °C)

chemical shifts reported in the literature[28] were as follows: δ 0.97 (d, 12H **(A)**, ^3J = 6.8

Hz), 1.23 (d, 12H **(C)**, ^3J = 6.8 Hz), 3.03 (sept, 4H **(B)**), 6.63 (d, 2H **(G)**, ^3J = 7.0 Hz),

7.26 (m(overlapping peaks), 6H **(D)**, **(E)**, **(F)**)), 7.36 (t, 2H **(H)**), 7.88 (d, 2H **(I)**, ^3J = 8.2

Hz). Further characterization of the ligand by IR (Nujol) revealed ν (C=N) and ν (C=C) at

1669, 1650 and 1641 cm^{-1}. The reported IR (KBr pellet) signals of this free ligand

reported in the literature were ν (C=N) cm^{-1} = 1668, 1651, 1640. The presence of the

starting diketone was ruled out because of the absence of ν (C=O) 1700-1800 at cm^{-1}.

2.2.1 Synthesis of (ArN=C(An)-C(An)=NAr)NiBr$_2$ (D) (Ar = 2,6-C$_6$H$_3$(^{i}Pr)$_2$, An = acenaphthene)
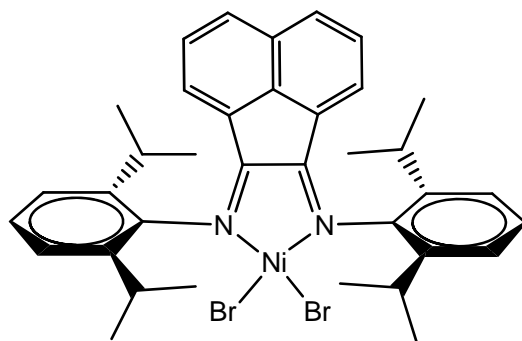
(D)

The precatalyst was synthesized following the procedure outlined in the literature.[26a] Dimethoxyethanenickel dibromide (1.0 g, 3.24 mmol, synthesized by literature procedure[29]) was added to the α-diimine ligand (1.70 g, 3.4 mmol) under an atmosphere of argon. To this was added 30 mL of dry CH$_2$Cl$_2$. The mixture formed a deep red/brown colour and was left stirring overnight at room temperature. The resulting red/brown powder was filtered, washed with ethyl ether and vacuum dried. Yield: 1.27 g, 54.6 %. The ^{1}H-NMR spectrum (Section 3.1.0.2, Figure 7-4) (CDCl$_3$, 300 MHz, 25 °C) exhibited resonances (slightly broadened singlets) with chemical shifts outside the normal spectral window: δ -16.0, 0.9, 1.6, 2.1, 5.3, 5.7, 17.3, 23.8 ppm. This is typical of a sample exhibiting paramagnetism,[26b] which may explain why no NMR data were given in the paper describing the preparation.[26a] In solution at room temperature the precatalyst is probably present as an equilibrium mixture of square planar (diamagnetic) and tetrahedral (paramagnetic) species.[26b]

2.3.0   Syntheses of trimethyl silyl ethers

2.3.0.1 Synthesis of (allyloxy)trimethylsilane (CH$_2$=CHCH$_2$OSiMe$_3$)
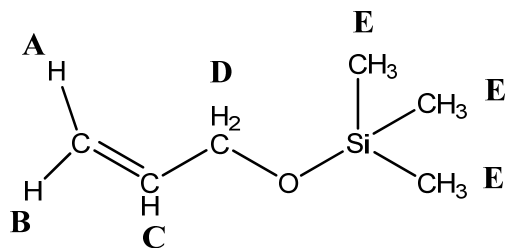
This compound was synthesized according to the literature procedure.[30a] To a mixture of hexamethyldisilazane (HMDS) (6.02 mL, 28 mmol) and LiClO$_4$ (2.24 g, 20 mmol) was added the allyl alcohol (2.75 mL, 40 mmol), and the mixture was stirred at room temperature under argon for 24 h. CH$_2$Cl$_2$ was then added, LiClO$_4$ was removed by filtration and the excess HMDS and the CH$_2$Cl$_2$ were removed under reduced pressure. The resulting product was purified, eluting through a short alumina chromatograph column with ethyl ether, which was subsequently removed under reduced pressure. Yield: 4.6972 g, 90 %. ^{1}H-NMR (Figure 8-1, 400 MHz, C$_6$D$_5$Cl, 25 °C): δ 0.20 (s, 9H **(E)**), 4.16 (d, 2H **(D)**, ^3J = 6.2 Hz), 5.12 (dd, 1H **(B)**, ^2J (*geminal*) = 2.1, ^3J (*cis*) = 10.3 Hz), 5.37 (dd, 1H **(A),** ^2J (*geminal*) = 2.1, ^3J (*trans*) = 16.8 Hz), 5.97 (m, 1H **(C)**, ^3J = 6.2, ^3J (*trans*) = 16.8, ^3J (*cis*) = 10.3 Hz). Literature (CDCl$_3$) δ 0.21 (s, 9H **(E)**), 4.46 (d, 2H **(D)**, ^3J = 6.2 Hz), 5.28 (dd, 1H **(B)**, ^2J (*geminal*) = 2.1, ^3J (*cis*) = 10 Hz), 5.42 (dd, 1H **(A),** ^2J (*geminal*) = 2.1, ^3J (*trans*) = 16.8 Hz), 6.06 (m, 1H **(C)**, ^3J = 6.2, ^3J (*trans*) = 16.8, ^3J (*cis*) = 10 Hz).

25

2.3.0.2 Synthesis of (but-3-enyloxy)trimethylsilane (CH₂=CH(CH₂)₂OSiMe₃)
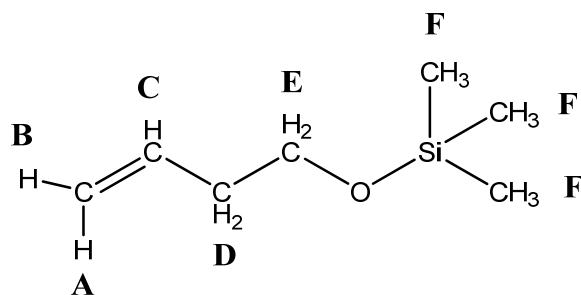
This compound was synthesized according to the literature procedure.[30a] To a mixture of hexamethyldisilazane (HMDS) (15.0 mL, 0.07 mol) and $LiClO_4$ (5.60 g, 0.05 mol) was added the 3-buten-1-ol (8.9 mL, 0.1mol), and the mixture was stirred at room temperature under argon for 24 hrs. CH_2Cl_2 was then added, $LiClO_4$ was removed by filtration and the excess HMDS and the CH_2Cl_2 were removed under reduced pressure. The resulting product was purified, eluting through a short alumina chromatograph column (6 - 7 cm) with ethyl ether, which was subsequently removed under reduced pressure. Yield: 10.7 g, 74 %. ^{1}H-NMR (Figure 9-1, 300 MHz, CDCl₃, 25 °C): δ 0.13 (s, 9H **(F)**, 2.30 (dt, 2H **(D)**, ^3J = 6.9, 6.2 Hz), 3.65 (t, 2H, **(E)**, ^3J = 6.9 Hz), 5.04 (dd, 1H **(B)**, ^2J (*geminal*) = 2.1, ^3J (*cis*) = 10.2 Hz), 5.09 (dd, 1H **(A)**, ^2J (*geminal*) = 2.1, ^3J (*trans*) = 16.8 Hz), 5.82 (m, 1H **(C)**, ^3J = 6.2, ^3J (*trans*) = 16.8, ^3J (*cis*) = 10.2 Hz)). The synthesis of (but-3-enyloxy)trimethylsilane has been cited in the literature, but no spectroscopic data were reported.[30c] Therefore, this is the first reported ^{1}H-NMR spectrum.

2.3.0.3 Synthesis of (dec-9-enyloxy)trimethylsilane (CH$_2$=CH(CH$_2$)$_8$OSiMe$_3$)
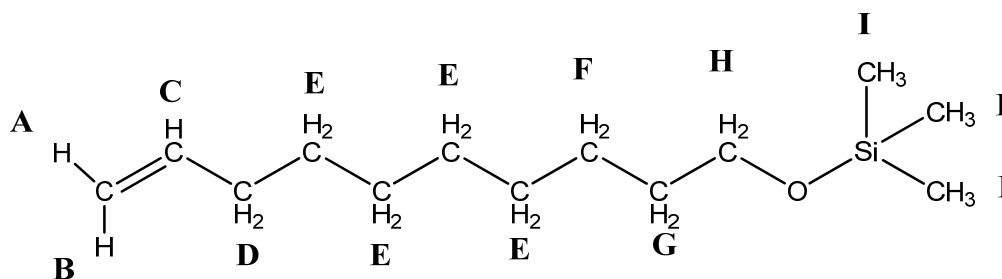
This compound was synthesized by Gregory Vettese according to the literature procedure.[31a] To a stirred solution of 9-decen-1-ol (19.6 mmol) and LP-SiO$_2$ (lithium perchlorate (1 g) dispersed unto SiO$_2$ (2 g)) in CH$_2$Cl$_2$ (10 mL), HMDS (11.5 mmol) was added and stirred overnight under an inert atmosphere. CH$_2$Cl$_2$ (10 mL) was then added, LP-SiO$_2$ was removed by filtration and the excess HMDS and the CH$_2$Cl$_2$ were removed under reduced pressure. The resulting product was purified, eluting through a short alumina chromatograph column with ethyl ether, which was subsequently removed under reduced pressure. ^{1}H-NMR (Figure 10-1, 300 MHz, CDCl$_3$, 25 °C): δ 0.11 (s, 9H **(I)**), 1.30 (m, 8H **(E)**), 1.38 (m, 2H **(F)**), 1.53 (m, 2H **(G)**), 2.04 (dt, 2H **(D)**, ^3J = 7.1, 6.2 Hz), 3.58 (t, 2H **(H)**, ^3J = 6.7 Hz), 4.93 (dd, 1H **(A)**, ^2J (*geminal*) = 2.1, ^3J (*cis*) = 10.2 Hz), 5.00 (dd, 1H **(B)**, ^2J (*geminal*) = 2.1, ^3J (*trans*) = 16.8 Hz), 5.82 (m, 1H **(C)**, ^3J = 6.2, ^3J (*trans*) = 16.8, ^3J (*cis*) = 10.2 Hz). Literature (CDCl$_3$)[31c] δ 0.08 (s, 9H **(I)**), 1.27 (m, 8H **(E)**), 1.33 (m, 2H **(F)**), 1.51 (m, 2H **(G)**), 2.01 (dt, 2H **(D)**), 3.54 (t, 2H **(H)**, ^3J = 7 Hz), 4.89 (d, 1H **(A)**, ^3J (*cis*) = 11 Hz), 4.96 (d, 1H, **(B)**, ^3J (*trans*) = 17 Hz), 5.77 (ddt, 1H **(C)**, ^3J = 7, ^3J (*trans*) = 17, ^3J (*cis*) = 10 Hz).

2.3.1 General Purity Test for Polar Monomers

Residual protic content of the polar monomers was checked by preparing a
solution in C_6D_6 of Cp_2ZrMe_2 in an NMR tube, and then adding the desired comonomer
(10 molar equivalents).[31b] The ^{1}H-NMR spectrum was then analyzed for the absences of
new Cp resonances (δ 5.74 ppm) from the formation of the hydrolysis product
$(Cp_2ZrMe)_2O$ and the production of methane (δ 0.24 ppm). The presence of the Zr-Me
resonance (δ -0.14 ppm) was also checked.[31b]

2.4.0 Homopolymerization Studies of Ethylene

2.4.0.1 General Procedure for Homopolymerizations

The following procedure describes a typical experiment for the
homopolymerization of ethylene. All modifications from this procedure are appropriately
noted.

To a flame-dried 100 mL Schlenk flask were added 10 mg of dibromo[1,4-
bis(2,6-diisopropylphenyl)acenaphthenediimine]nickel(II) and 30 mL of dry toluene.
Ethylene (1 atm) was then bubbled into this solution for 5 min, saturating the
precatalyst/toluene solution. MAO (1000 equiv, 10 wt % in toluene) was then added to
the Schlenk flask and the mixture was stirred for 30 min while bubbling of ethylene was
continued. The reaction was then quenched with 200-300 mL of methanol/HCl solution
and the resulting mixture was stirred overnight. The precipitated polymers were then
filtered, washed with methanol and dried under vacuum at 60 ºC overnight. The
homopolymers were then analyzed by ^{1}H-NMR, IR spectroscopy and, where possible, by
differential scanning calorimetry.

2.4.1   Copolymerization Studies of Ethylene with Polar Monomers

2.4.1.0 General Procedure for Copolymerizations

The following procedure describes a typical experiment for the copolymerization of ethylene with the polar monomers. All modifications from this procedure are appropriately noted.

To a flame-dried 100 mL Schlenk flask were added 10 mg of dibromo[1,4-bis(2,6-diisopropylphenyl)acenaphthenediimine]nickel(II) and 15 mL of dry toluene. The desired comonomer (100 equiv) in 15 mL of dry toluene was added to the precatalyst/toluene solution and the mixture was stirred for 10 min. Ethylene (1 atm) was bubbled into this solution for 5 min to saturate the precatalyst/comonomer/toluene solution. MAO (1000 equiv, 10 wt % in toluene) was added to the Schlenk flask and the solution was stirred for 30 min while bubbling of ethylene was continued. The copolymerization was quenched with 200-300 mL of an ethanol/HCl or methanol/HCl solution and the resulting mixture was stirred overnight. The precipitated copolymers were then filtered, washed with methanol/ethanol and dried under vacuum at 60 ºC overnight. The precipitated copolymers were then analyzed by ^{1}H-NMR and IR spectroscopy and, where possible, by differential scanning calorimetry.

Chapter 3.   Results and Discussion

3.1.0   Syntheses of ligand and precatalyst

3.1.0.1 Synthesis of [N'N-(2,6-diisopropylphenyl)imino]acenaphthene

This ligand was synthesized via an acid catalyzed condensation reaction outlined
in the literature[28] (Figure 7-1).
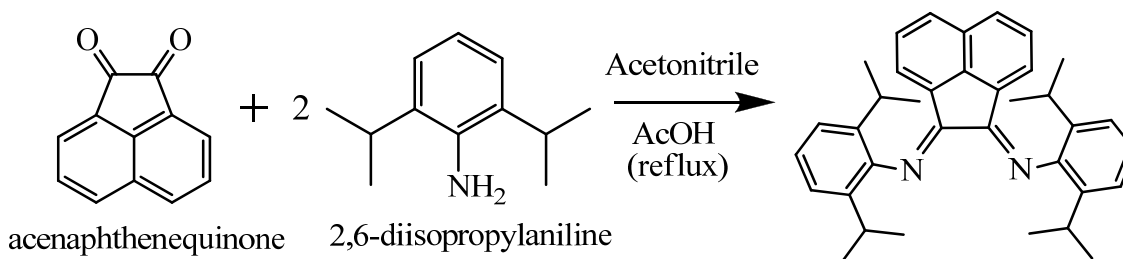
Figure 7-1: Synthesis of [N'N-(2,6-diisopropylphenyl)imino]acenaphthene

Figure 7-2 below shows the ^{1}H-NMR obtained from the pure ligand. This provided
evidence that the desired yellow-coloured ligand was synthesized after comparing the
experimental chemical shifts and coupling constants with those in the literature.[28] The
two methyl groups of each isopropyl group are inequivalent.
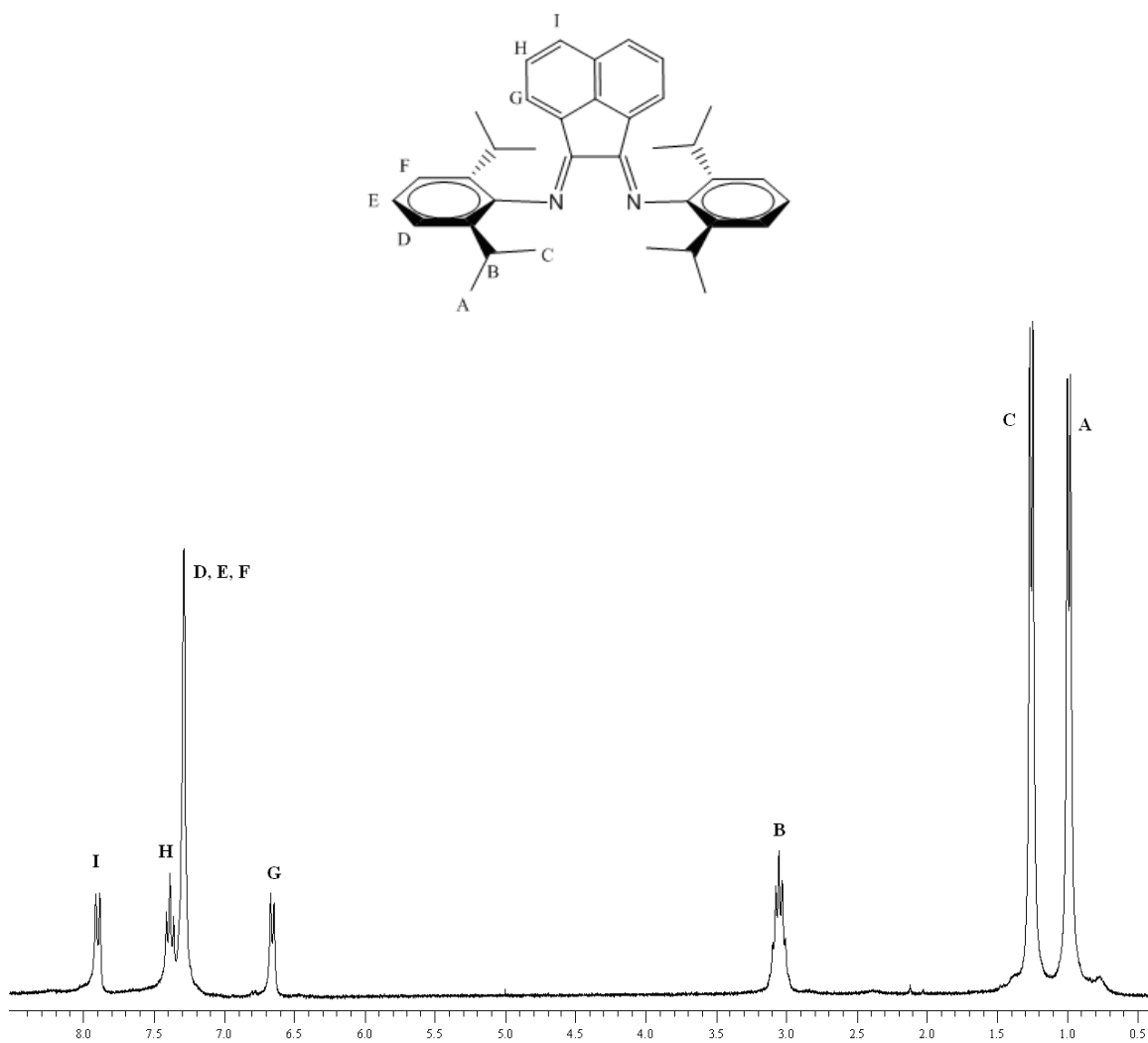
Figure 7-2: ^{1}H-NMR spectrum (HM-035, CDCl$_3$, 300MHz, 25 ºC) of [N'N-(2,6-diisopropylphenyl)imino]acenaphthene

3.1.0.2 Synthesis of dibromo[1,4-bis(2,6-diisopropylphenyl)acenaphthenediimine]-nickel(II) (D)

The precatalyst was synthesized following the procedure outlined in the literature[26a], shown in Figure 7-3.
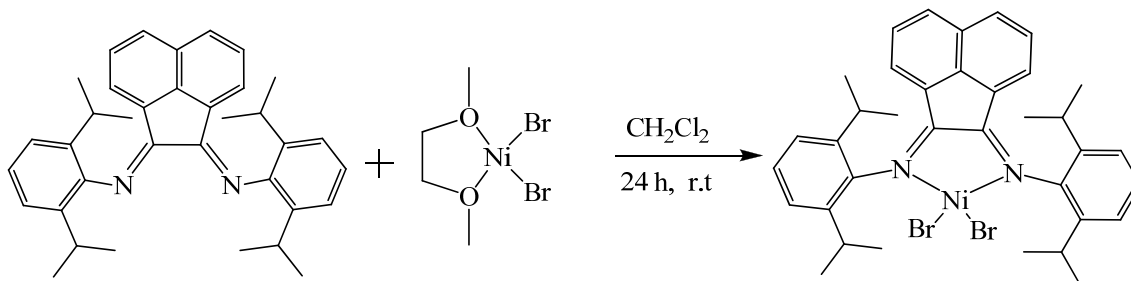
Figure 7-3: Synthesis of dibromo[1,4-bis(2,6-diisopropylphenyl)acenaphthenediimine]nickel(II)

This reaction was very effective as it involved the substitution of the very labile dimethoxyethane ligand with the α-diimine ligand. In the literature[26a] elemental analysis was the only technique used to characterize this compound and further analysis seemed appropriate. The ^{1}H-NMR spectrum shown in Figure 7-4 provides evidence of interesting characteristics. The chemical shifts (*) outside the normal spectral window (δ -16.0, 17.3, 23.8) demonstrated that the sample exhibits paramagnetism.[26b] In solution at room temperature the precatalyst is probably present as an equilibrium mixture of square planar (diamagnetic) and tetrahedral (paramagnetic) species.[26b] At -70 ºC similar resonances were also exhibited in the ^{1}H-NMR spectrum (Figure 7-5, CD$_2$Cl$_2$, 600 MHz, -70 ºC: δ -12.2, 0.8, 1.2, 1.6, 1.9, 4.6, 8.6, 14.6, 18.8, 23.2, 23.7, 27.7). As reported in the literature, this is quite characteristic of some nickel(II), d^8 systems.[26b]
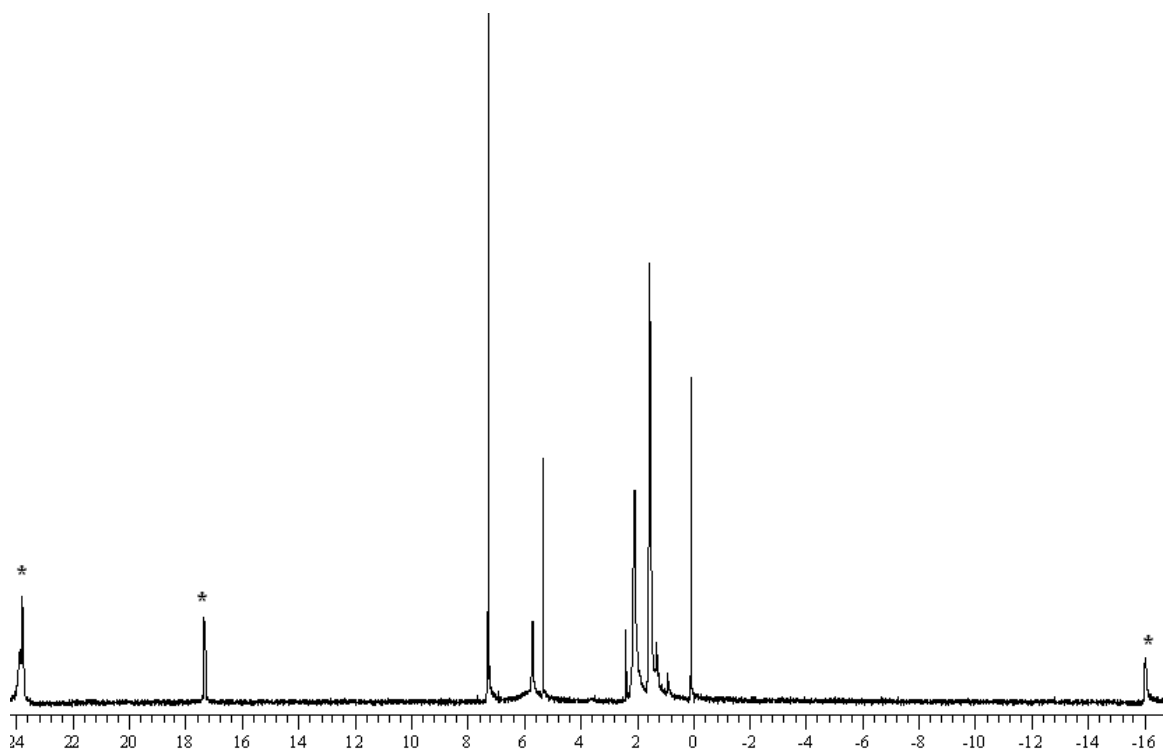
Figure 7-4: ^{1}H-NMR spectrum (HM-037, expt. 37, CDCl$_3$, 300 MHz, 25 ºC) of precatalyst
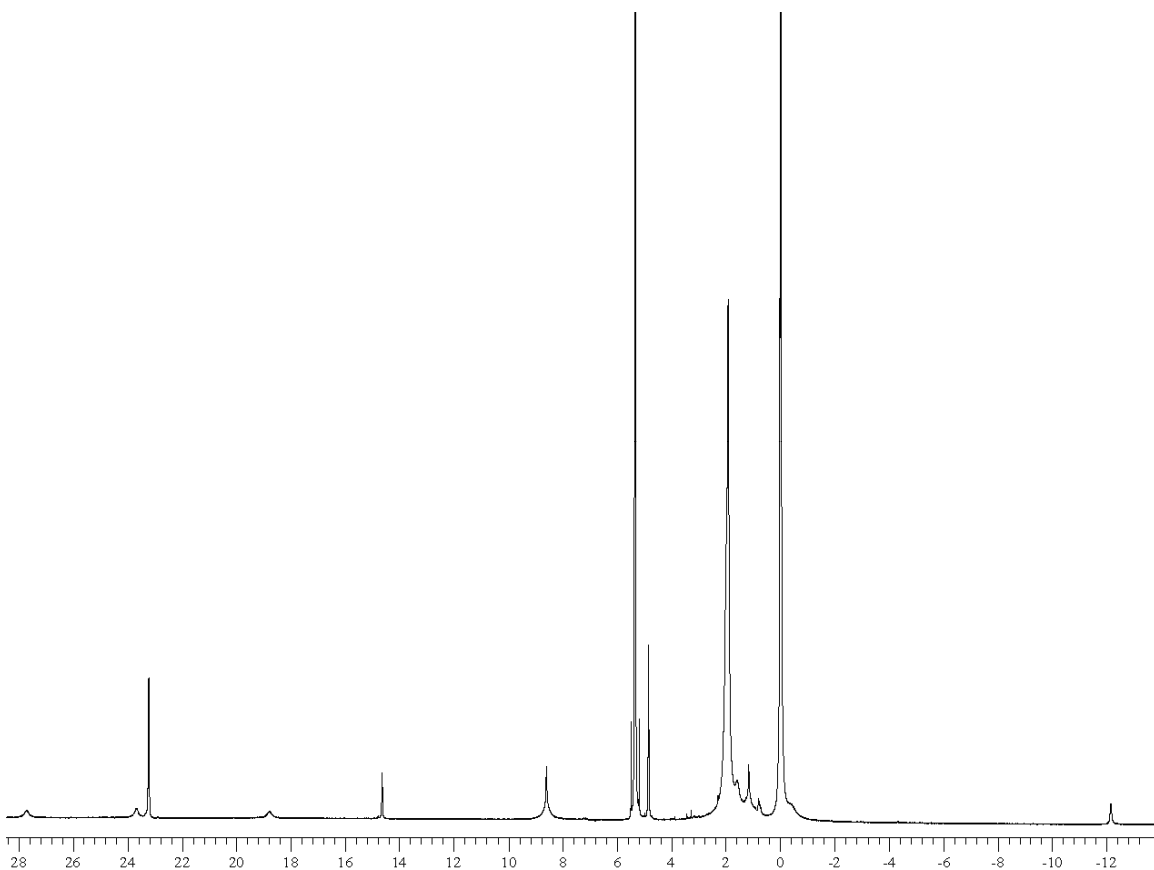
Figure 7-5: ^{1}H-NMR spectrum (HM-050, expt. 3, CD$_2$Cl$_2$, 600 MHz, -70 ^{o}C) of precatalyst

3.2.0   Synthesis of polar monomers

(Allyloxy)trimethylsilane and (but-3-enyloxy)trimethylsilane were synthesized following the procedure outlined in the literature (Figure 7-6).[30a] (Dec-9-enyloxy)trimethylsilane was synthesized by a fellow coworker, Gregory Vettese.
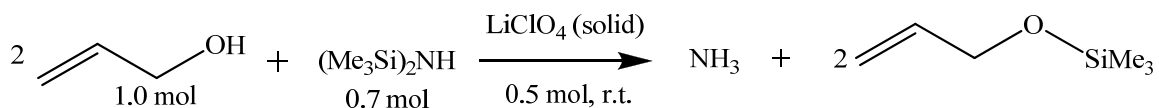
Figure 7-6: Pathway for polar monomer synthesis

This method provided a very efficient and effective way of synthesizing (allyloxy)trimethylsilane and (but-3-enyloxy)trimethylsilane using solvent free conditions. Hexamethyldisilazane (HMDS) is used as the silylation agent, but he actual mechanism by which $LiClO_4$ catalyzes the reaction is unknown. This reaction is very clean as ammonia is the only byproduct and is easily removed, and the catalyst ($LiClO_4$) is easily recovered by filtration.

The ^{1}H-NMR spectra in Figures 8-1, 9-1 and 10-1 shows that the desired comonomers were synthesized upon comparison of the reported chemical shifts with the literature. The results obtained from the purity test with Cp_2ZrMe_2 are shown in Figures 8-2, 9-2 and 10-2. Based on the single chemical shifts obtained for the Zr-Cp and Zr-Me resonances at δ 5.7 and δ -0.14 respectively, hydrolysis (cleavage of the Zr-Me) of Cp_2ZrMe_2 had not occurred, showing an absence of hydroxyl impurities (water or unreacted alcohol).
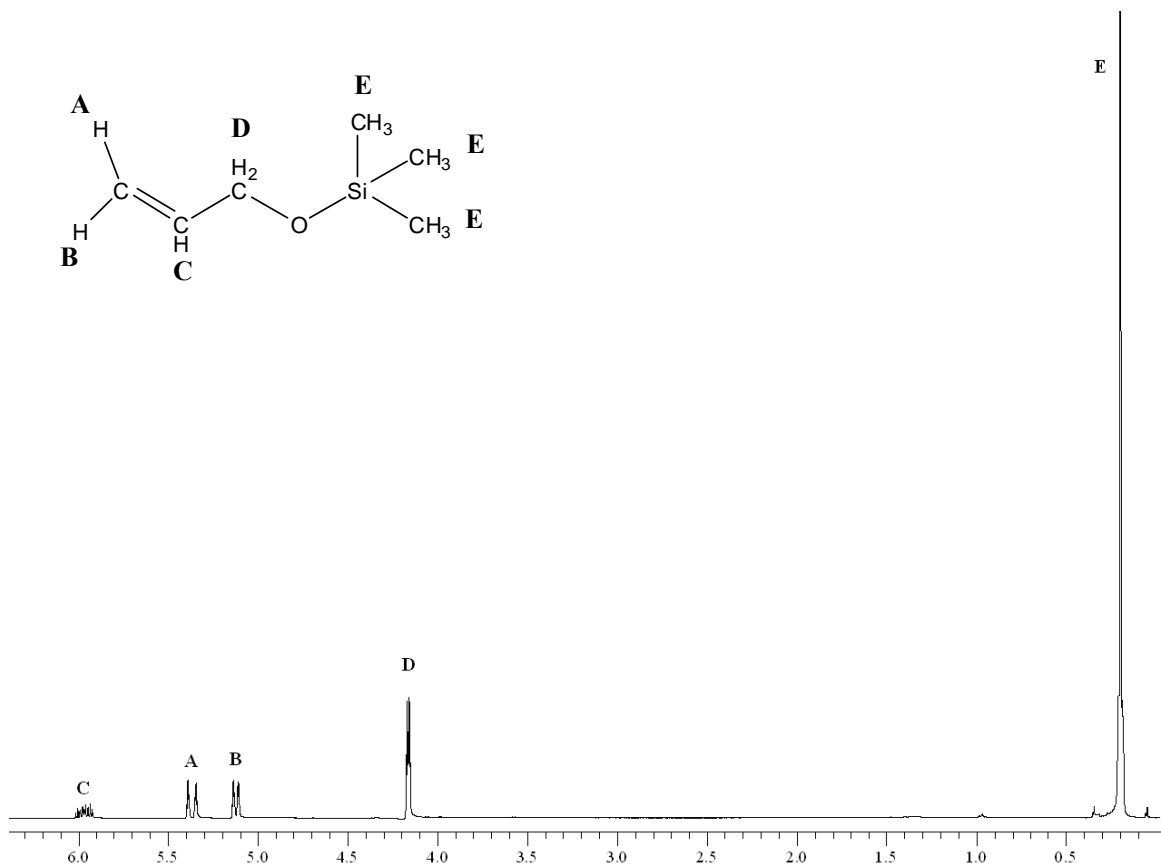
Figure 8-1: ^{1}**H-NMR spectrum (HM-041, expt. 4, 400 MHz, C$_6$D$_5$Cl, 25 ºC) of (allyloxy)trimethylsilane**
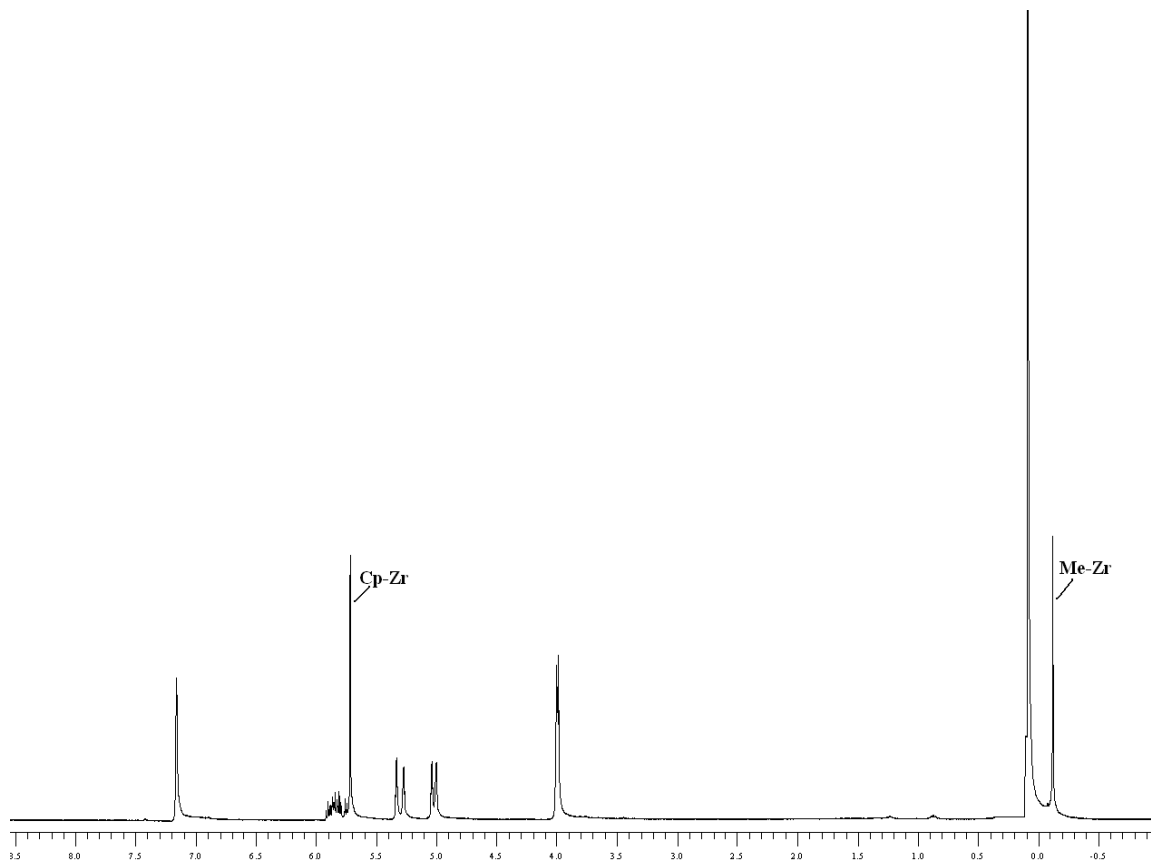
Figure 8-2: ¹H-NMR spectrum (HM-040, expt. 1, 300 MHz, C₆D₆, 25 ºC) of (allyloxy)trimethylsilane test with Cp₂ZrMe₂
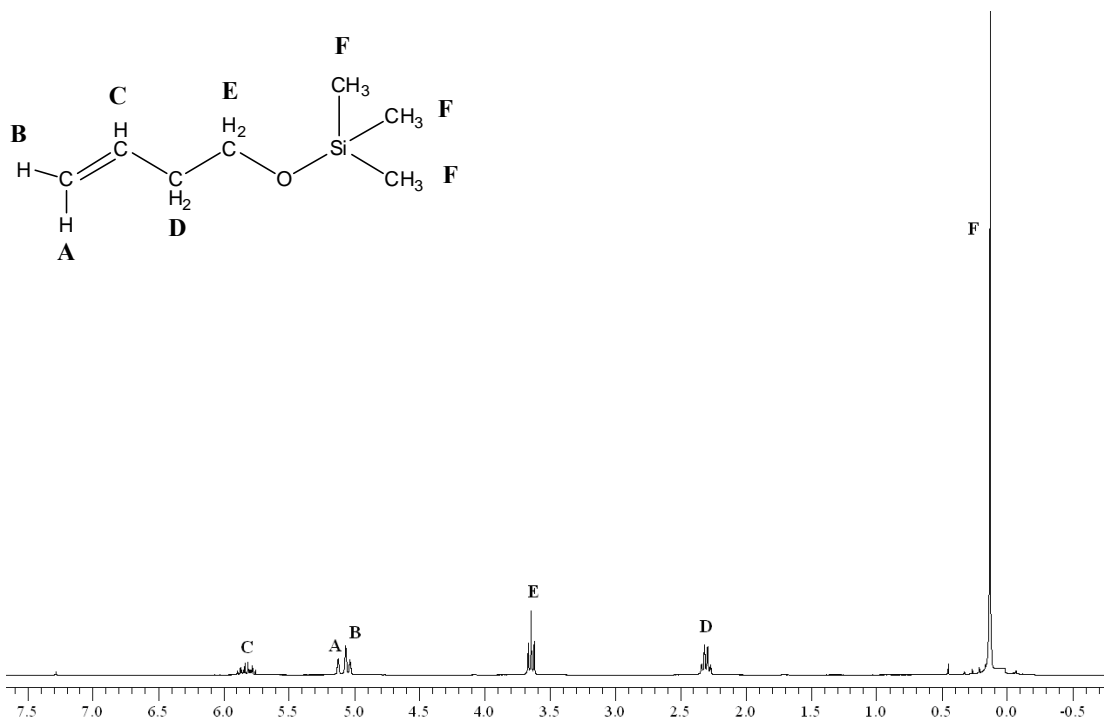
Figure 9-1: ^{1}H-NMR spectrum (HM-048, expt. 3, 300 MHz, CDCl$_3$, 25 ^{o}C) of (but-3-enyloxy)trimethylsilane
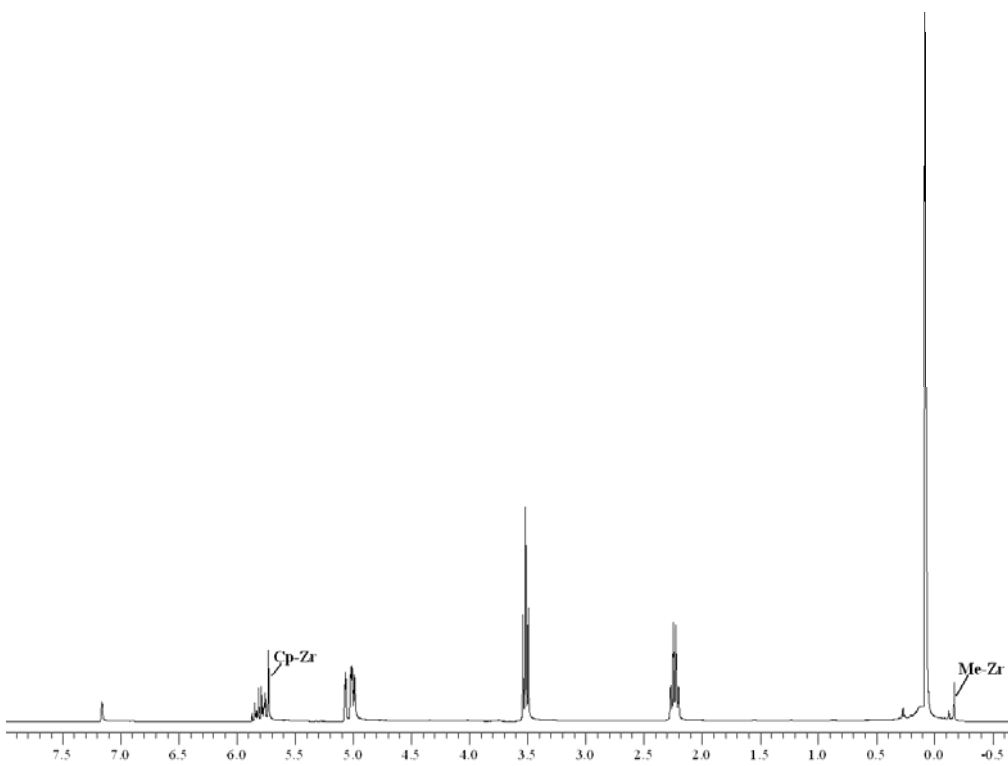
Figure 9-2: ^{1}H-NMR spectrum (HM-048, expt. 5, 300 MHz, C$_6$D$_6$, 25 ^{o}C) of (but-3-enyloxy)trimethylsilane test with Cp$_2$ZrMe$_2$
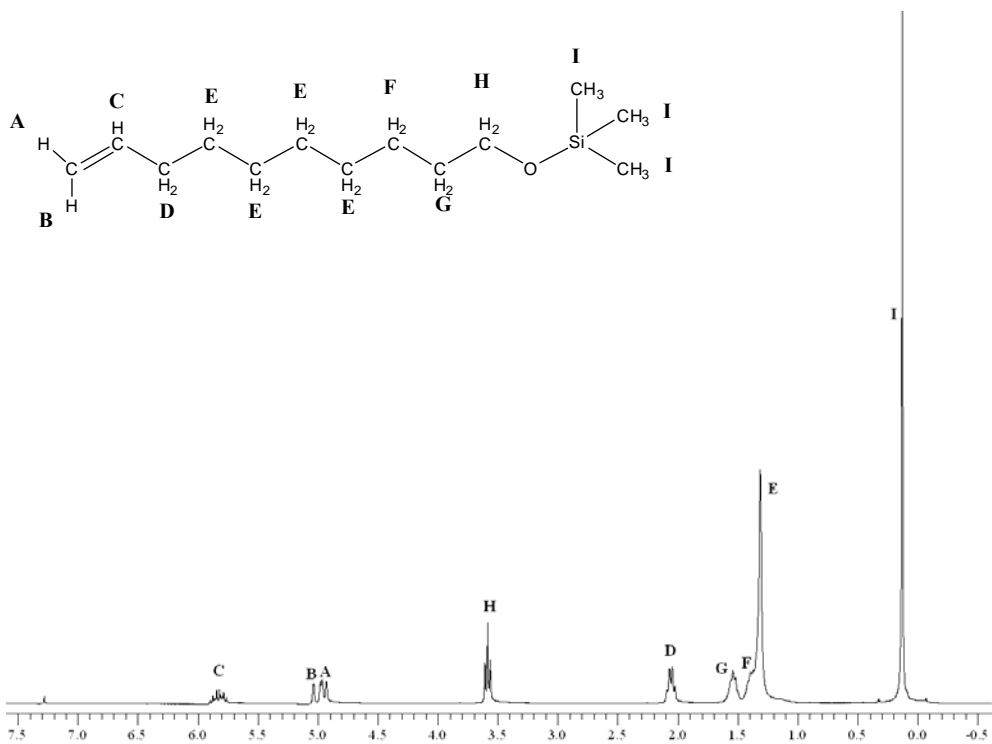
Figure 10-1: ^{1}H-NMR spectrum (HM-050, expt. 1, 300 MHz, CDCl$_3$, 25 ^{o}C) of (dec-9-enyloxy)trimethylsilane
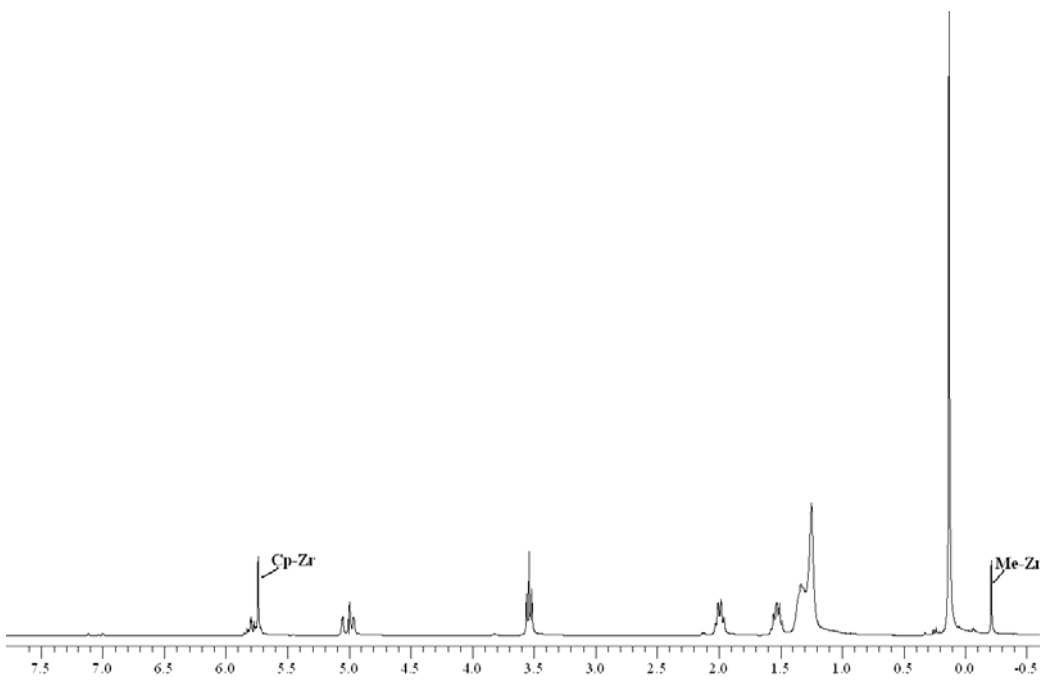
Figure 10-2: ^{1}H-NMR spectrum (HM-050, expt. 5, 300 MHz, C$_7$D$_8$, 25 ^{o}C) of (dec-9-enyloxy)trimethylsilane test with Cp$_2$ZrMe$_2$

3.3.0 Homopolymerization of ethylene

All ethylene homopolymerizations followed the reaction pathway outlined in equation 3-0 below. Generally, 10 mg of dibromo[1,4-bis(2,6-diisopropylphenyl)acenaphthenediimine]nickel(II) was added to a flame-dried 100 mL Schlenk flask and 30 mL of dry toluene was added. Ethylene (1 atm) was then bubbled into this solution for 5 min, saturating the precatalyst/toluene solution. MAO (1000 equiv, 10 wt % in toluene) was then added to the Schlenk flask and the mixture was stirred for 30 min while bubbling of ethylene was continued. The reaction was then quenched with 200-300 mL of methanol/HCl solution and the resulting mixture was stirred overnight. The precipitated polymers were then filtered, washed with methanol and dried under vacuum at 60 ℃ overnight. As mentioned in Section 1.1.2 the polymers produced by late transition metal catalyst systems have random branches of varied lengths along the backbone.[4c]

$$\text{Catalyst (D)/MAO} \over \text{Toluene, 1 atm}$$

eq. 3-0
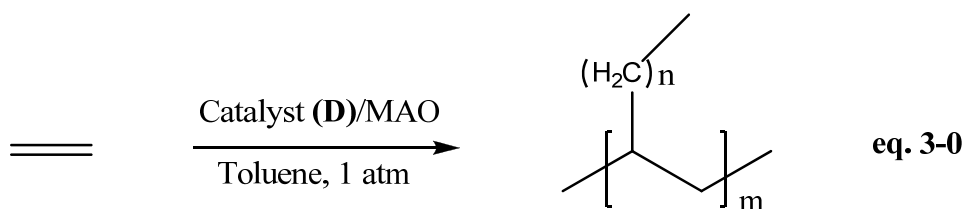
Upon analyses of the ^{1}H-NMR spectra, a better understanding of how the polymer microstructure changes by varying the reaction conditions was obtained. Additional information was also obtained from the IR spectra and differential scanning calorimetric analyses. Figure 11-1 shows a representative ^{1}H-NMR spectrum of the type of polyethylene obtained at ambient temperature and 1 atm.
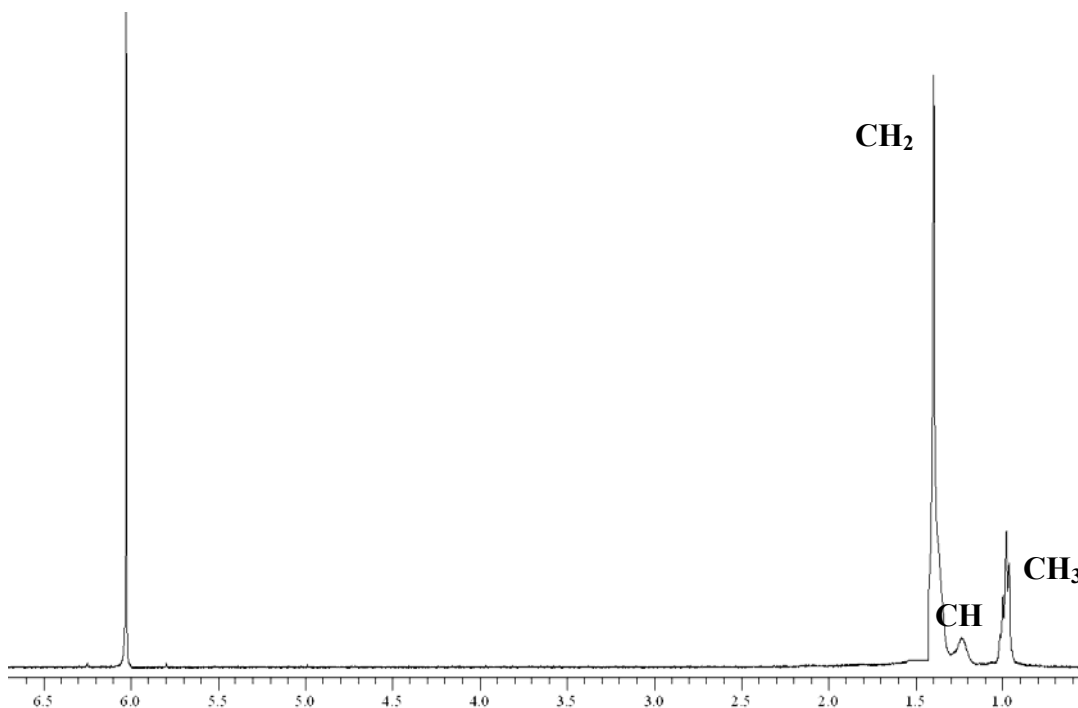
Figure 11-1: ^{1}H-NMR spectrum (Run 8, 400 MHz, TCE-d$_2$, 120 °C) of polyethylene

Experimentally 74 (Run 1) branches per 1000 carbon atoms were obtained. This was comparable to the 71 obtained by Brookhart *et al.*[26a] To determine the number of branching carbon atoms per 1000 carbons (degree of branching) within the polyethylene backbone, equations 3-1, 3-2 and 3-3 are used. These equations require the area (integration) under the CH (δ 1.2), CH$_2$ (δ 1.4) and CH$_3$ (δ 0.9) peaks obtained from the ^{1}H-NMR spectra. Equations 3-1, 3-2 and 3-3 are provided below.

Total # of carbon atoms in an average polymer chain

= [(CH integration)/1 + (CH$_2$ integration)/2 + (CH$_3$ integration)/3]   **eq. 3-1**

Fraction of branching carbons = [(CH integration)/1] / total # of carbon atoms   **eq. 3-2**

# of branches per 1000 C = fraction of branching carbons x 1000   **eq. 3-3**

Figure 11-2 shows a representative IR spectrum of the polyethylene obtained using this catalytic system. It exhibited the characteristic C-H stretches of the polymer backbone at 2900-2850 cm^{-1}. The C-H bending modes were also present at 1470 and 1375 cm^{-1}.[32]
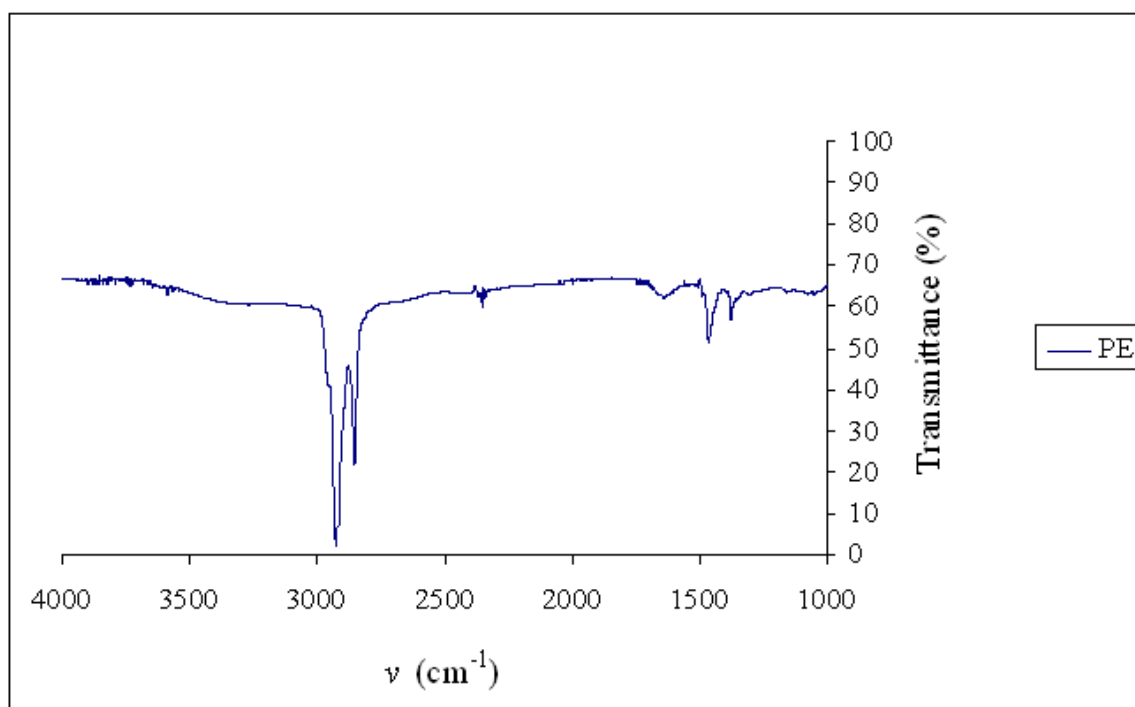
Figure 11-2: Transmittance infrared spectrum (film) of polyethylene (Run 7)

Table 1: Preliminary results of the homopolymerization of ethylene.[a]

Run	MAO (equiv.)	Moles of precatalyst ($\times 10^6$)	Initial Temperature (°C)	Yield (g)	Catalyst Activity (kg/mol)	Branches per 1000 C[a]
1	1000	14	25	2.2	160	74
2	1000	14	25	1.8	130	142
3	500	15	25	2.3	150	115
8	1000	14	25	2.1	150	162
7	1000	14	0	2.2	160	205
9	1000	14	60	1.9	140	170

[a] All polymerization reactions were run for 30 min. [b] Determined from ^{1}H-NMR spectra analyses using equations 3-1, 3-2 and 3-3. [Ethylene] is 0.13 M and 0.08 M at 25 °C and 60 °C respectively.[30b]

There was an overall lack of reproducibility with the homopolymerizations. Despite repeated attempts at duplicating the reaction conditions (Run 1 and Run 2) the type of polymers produced had different microstructures (degree of branching) each time. Thus there were no overall trends with respect to the catalyst activity, catalyst loading or reaction temperature. However, Brookhart and his coworkers found that as the initial temperature of the reaction increased catalyst activity decreased.[26a] This demonstrates the unpredictable nature of these processes. As mentioned in Section 1.5.1, an increase in the degree of branching was expected as the temperature was increased. However, the highest degree of branching was obtained at 0 °C.

It was also interesting that upon comparing runs 3 and 8 (Table 1), the catalyst activity was unaffected by an increase in the catalyst loading or a reduction in the MAO

equiv. This shows that there was no linear correlation with the amount of catalyst used and the catalyst's activity.

3.4.0   Copolymerization of ethylene with polar monomers

All ethylene copolymerizations followed the reaction pathway outlined in equation 3-4 below. To a flame-dried 100 mL Schlenk flask were added 10 mg of dibromo[1,4-bis(2,6-diisopropylphenyl)acenaphthenediimine]nickel(II) and 15 mL of dry toluene. The desired comonomer in 15 mL of dry toluene was added to the precatalyst/toluene solution and the mixture was stirred for 10 min. Ethylene (1 atm) was bubbled into this solution for 5 min to saturate the precatalyst/comonomer/toluene solution. MAO (1000 equiv, 10 wt % in toluene) was added to the Schlenk flask and the solution was stirred for 30 min while bubbling of ethylene was continued. The copolymerization was quenched with 200-300 mL of an ethanol/HCl or methanol/HCl solution and the resulting mixture was stirred overnight. The precipitated copolymers were then filtered, washed with methanol/ethanol and dried under vacuum at 60 °C overnight. The resulting copolymers were analyzed by DSC (where possible), ^{1}H-NMR and IR spectroscopy.
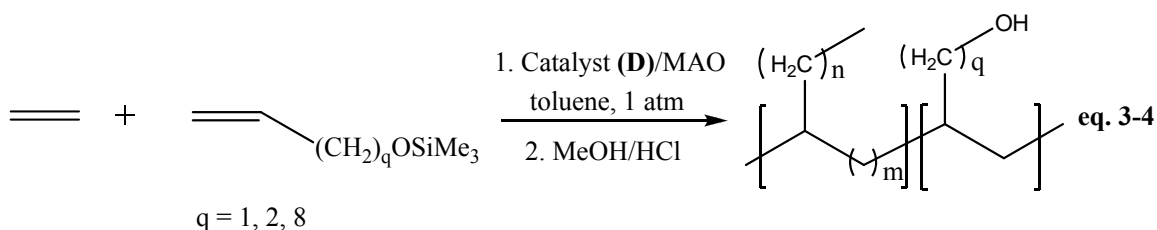
The copolymers were obtained by the hydrolysis of the siloxy groups. This yielded LLDPE with C_1, C_2 and C_8 branches containing OH end groups. The mechanism of the acid catalyzed hydrolysis is outlined below.

The siloxy group is first protonated by HCl followed by the desilylation by water forming protonated hydroxy trimethylsilane and the deprotected copolymer with random branches having –OH end groups.
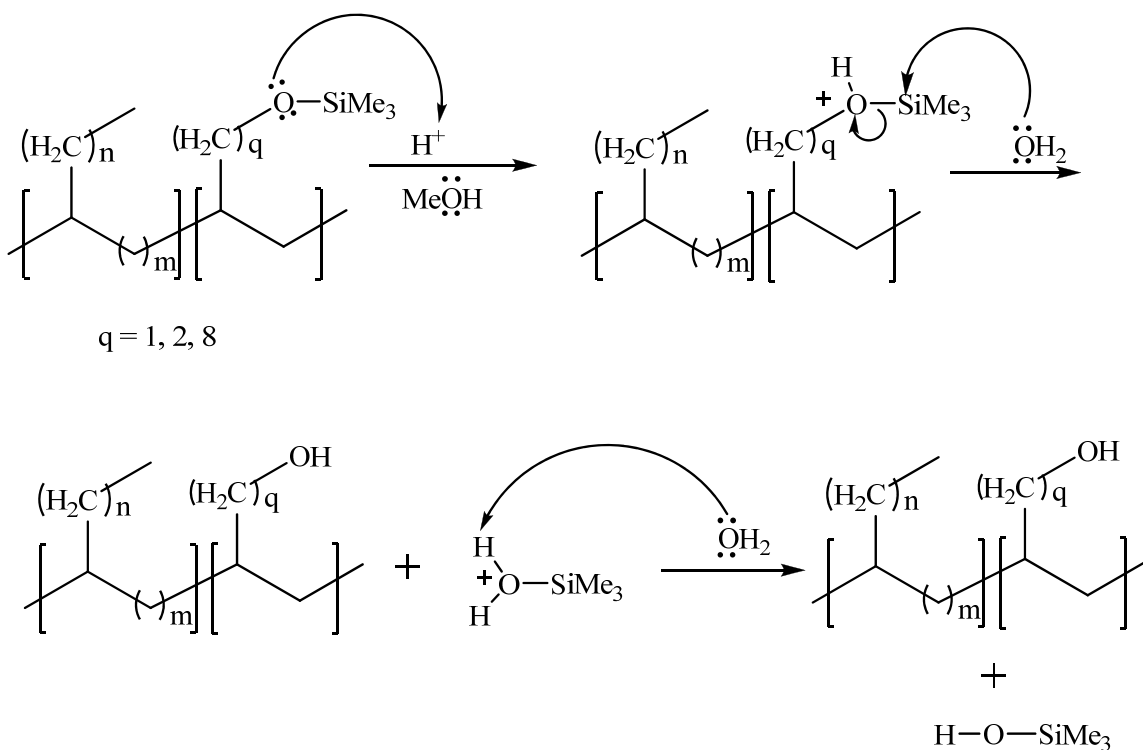
Figure 12-1: Reaction pathway for the deprotection of the siloxy protecting group via hydrolysis

3.4.1   Copolymerization with (allyloxy)trimethylsilane

The resulting copolymers were analyzed by ^{1}H-NMR and IR spectroscopy and DSC analysis where possible. Figures 12-2, 12-3 and 12-4 show the ^{1}H-NMR spectra of poly(ethylene-*co*-allyl alcohol) with 0.66, 4.0 and 9.0 mol % incorporated allyl alcohol respectively. The doublet at δ 3.52 is attributable to the α-protons of the deprotected allyl alcohol side chains. The chemical shifts of the methylene protons of the main chain –$(CH_2)_n$- and the methyl -CH_3 end groups occurred at δ 1.4 and δ 0.9 respectively.[26c,d] On the basis of ^{1}H-NMR analyses it is impossible to determine whether or not the polymer samples are mixtures of homo- and copolymers. Therefore the percentage incorporations calculated are minimum values.
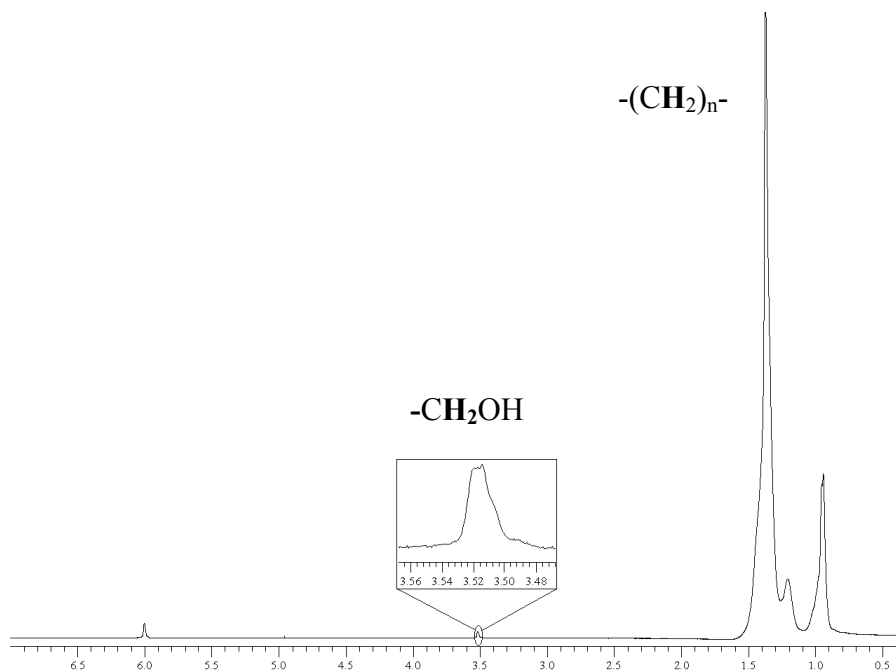
Figure 12-2: ^{1}H-NMR spectrum (Run 12, 0.66 mol%, 400 MHz, TCE-d$_2$, 120 ºC) of poly(ethylene-*co*-allyl alcohol)
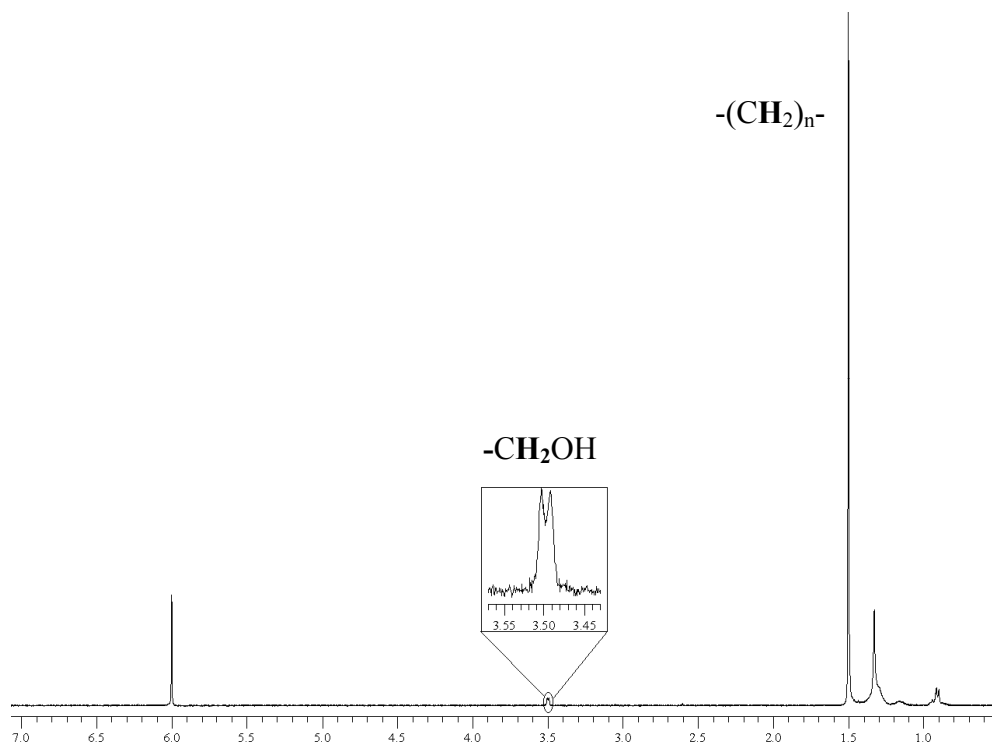
Figure 12-3: ^{1}H-NMR spectrum (Run 11, 4.0 mol%, 400 MHz, TCE-d$_2$, 120 ºC) of poly(ethylene-*co*-allyl alcohol)
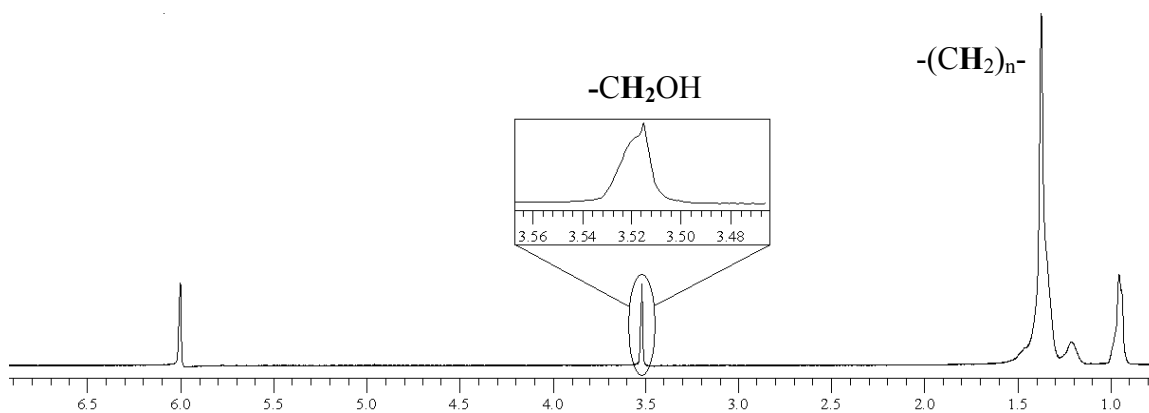
Figure 12-4: ^{1}H-NMR spectrum (Run 16, 9.0 mol%, 400 MHz, TCE-d$_2$, 120 ºC) of poly(ethylene-*co*-allyl alcohol)

To confirm the incorporation of the polar comonomer into the polymer main chain, the copolymers were further analyzed by IR spectroscopy. Figures 12-5, 12-6 and 12-7 show the IR spectra of poly(ethylene-*co*-allyl alcohol) obtained having 0.66, 4.0 and 9.0 mol % allyl alcohol incorporation respectively. Compared to the IR spectrum of the homopolymer (Figure 11-4) the copolymers have the characteristic –OH stretch around 3400 cm^{-1}, along with the C-H stretches at 2900-2850 cm^{-1} and the C-H bending modes at 1470 and 1375 cm^{-1}. The C-O stretches were also observed at 1122, 1119 and 1127 cm^{-1} in Figures 12-5, 12-6 and 12-7 respectively.[32] The relative intensities of the -OH stretches also increased as the mol % incorporation increased.
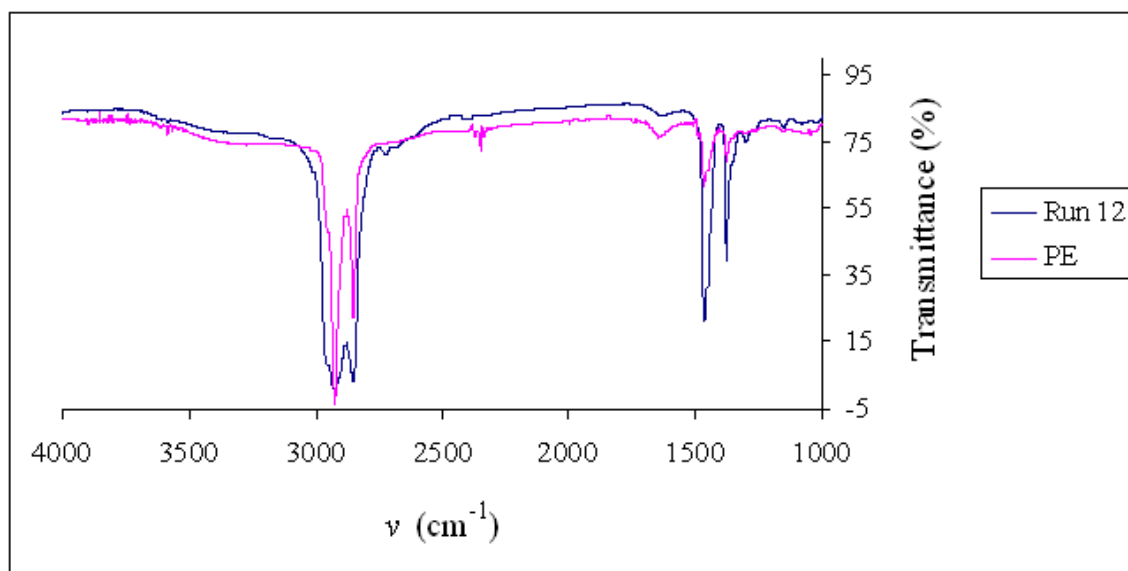
Figure 12-5: Transmittance infrared spectrum (film) of poly(ethylene-*co*-allyl alcohol)(Run 12, 0.66 mol%)
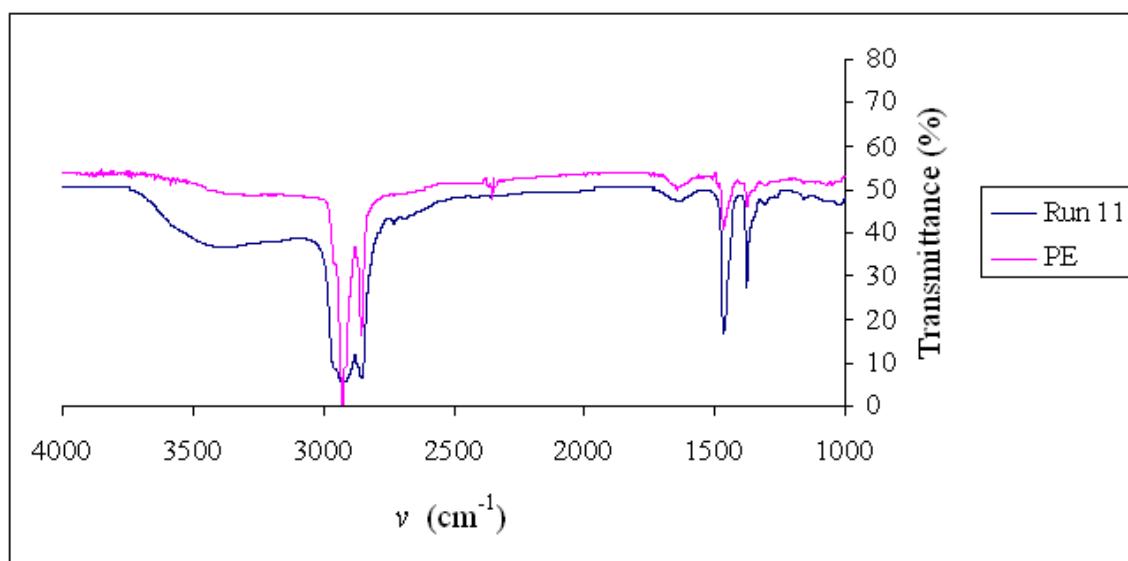
Figure 12-6: Transmittance infrared spectrum (film) of poly(ethylene-*co*-allyl alcohol)(Run 11, 4.0 mol%)
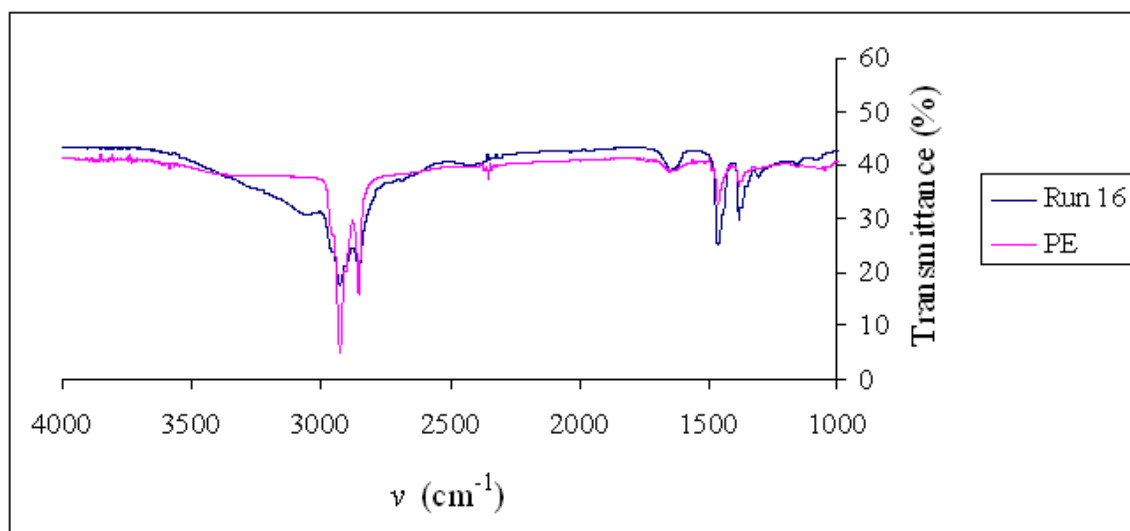
Figure 12-7: Transmittance infrared spectrum (film) of poly(ethylene-*co*-allyl alcohol)(Run 16, 9.0 mol%)

Table 2: Copolymerization results of poly(ethylene-*co*-allyl alcohol).[a]

Run	MAO (equiv.)	Moles of precatalyst ($\times 10^6$)	Comonomer (equiv.)	Initial Temp. (°C)	Yield (g)	Catalyst Activity (kg/mol)	Mol % incorp.[b]
10	1000	15	100	25	1.8	120	3.4
11	1000	19	100	25	3.9	200	4.0
12	1000	17	100	25	1.6	90	0.66
13	1000	15	50	25	4.1	270	0.00
14	1000	15	50	25	1.9	130	1.4
15	500	17	100	25	0.50	30	0.00
16	1000	17	50	0	1.5	90	9.0
17	1000	16	50	25	1.9	120	6.3
18	1000	15	50	60	0.08	10	0.00

[a] Copolymerizations were run for 30 min [b] Determined from ^{1}H-NMR spectra analyses using equation 3-5. [Ethylene] is 0.13 M and 0.08 M at 25 °C and 60 °C respectively.[30b]

The mole percent incorporations were determined using equation 3-5, where ACH_2O represents the integration of the α-proton (δ 3.52) from the allyl alcohol incorporated into the polyethylene backbone. $ACH_{2(PE)}$ represents the integration of the methylene protons (δ 1.4) from the polyethylene backbone (4 from ethylene plus 2 from allyl alcohol).

Mol % incorporation = $(ACH_2O/2) / [(ACH_{2(PE)} - ACH_2O)/4 + ACH_2O/2]$ **eq. 3-5***

* **Derivation of eq. 3-5 can be found in the appendix**

The results obtained from the copolymerizations with (allyloxy)trimethylsilane provided the most interesting results. Table 2 shows that the percentage incorporations ranged from 0.0 to 9.0 mol %. These results differed from those obtained from various researchers.[33] A metallocene (*rac*-Me$_2$Si(Ind)$_2$ZrCl$_2$) catalytic system was used; therefore different results were expected with this nickel(II) system. It was found that the comonomers with longer spacer groups between the oxygen atom and the double bond reported the highest degree of incorporations.[33] Other studies focused on the functionalization of polyethylene with allyl alcohol pretreated with trialkylaluminum.[34] A metallocene catalyst **(E)** (Figure 12-8) was used. Low incorporation (~ 1 mol %) was obtained with the smaller trialkylaluminum protecting groups (Me, Et) and it occurred predominantly at the chain end. Internal incorporation was reported with the bulkier protecting groups (triisobutylaluminum) however, still minimal.[34] Functionalization usually occurred predominantly at the chain end and the allyl alcohol was usually pretreated with bulky trialkyl aluminum masking agents. These studies demonstrated the challenges mentioned in the introduction and the need for extensive work in this area of research.

(E)
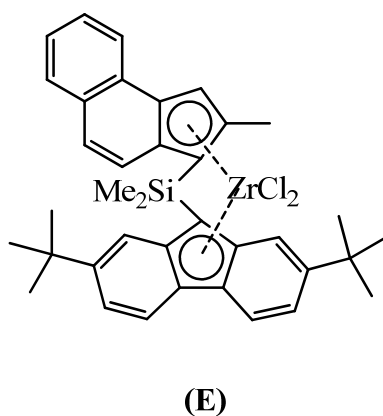
Figure 12-8: Metallocene precatalyst (E)

The copolymers were also analyzed by DSC to determine the melting temperatures. However, upon analysis of the DSC traces, no distinct T_m values were observed. This is very interesting as this shows that the copolymers produced were not very crystalline. This may be as a result of longer methylene branches along the polymer backbone affecting the crystal packing within the material. This overshadows the impact that the incorporated allyl alcohol branches (C_1) would have.

There are no overall trends with these copolymerizations (Table 2). Similar to the results obtained with the homopolymerizations (Table 1) there is a lack of reproducibility with these reactions (Run 13 and Run 14). It is interesting to note however that an unusually high percentage incorporation of 9.0 mol % (Run 16) was obtained. It also seems that an increase in temperature affects the incorporation of the comonomer (Run 18). However this is not a trend. Overall the results obtained from these copolymerizations provide further evidence that a lot more work is needed in this area to further understand how these systems work.

3.4.2 Copolymerization with (but-3-enyloxy)trimethylsilane

The resulting copolymers were analyzed by ^{1}H-NMR and IR spectroscopy and DSC analysis where possible. Figures 13-1 and 13-2 show the ^{1}H-NMR spectra of poly(ethylene-*co*-(but-3-enol)) with 3.0 and 9.8 mol % incorporated but-3-enol respectively.
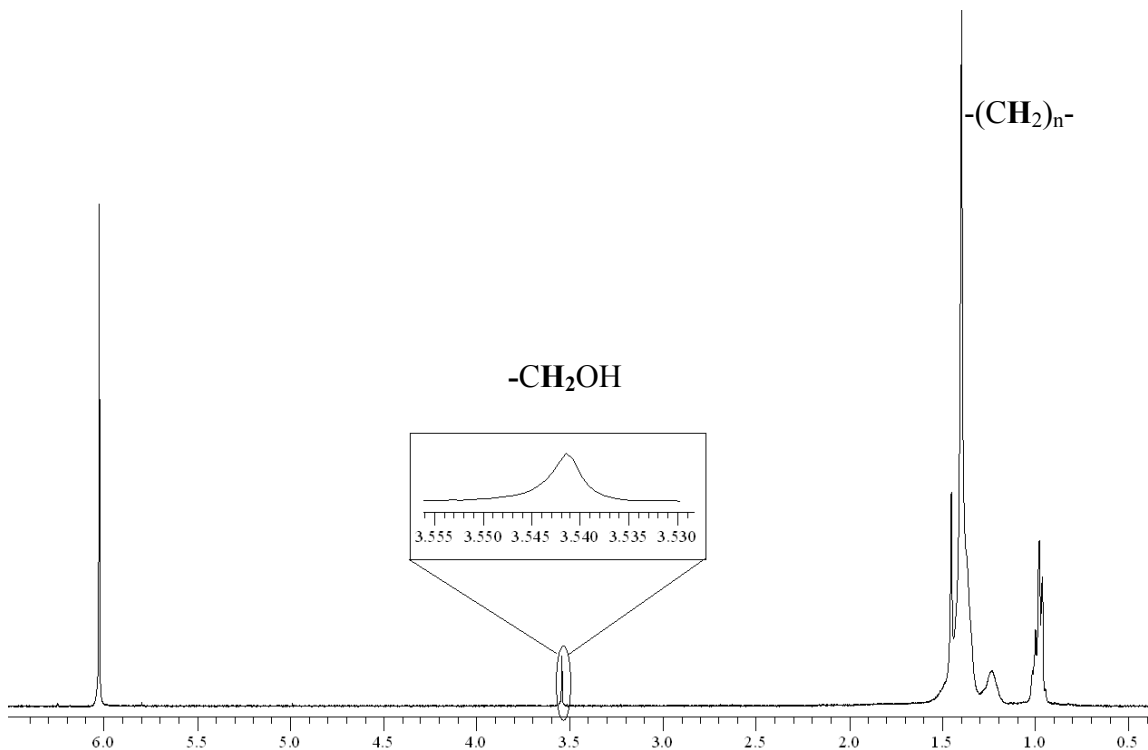
Figure 13-1: ^{1}H-NMR spectrum (Run 30, 3.0 mol %, 400 MHz, TCE-d$_2$, 120 ºC) of poly(ethylene-*co*-(but-3-enol))
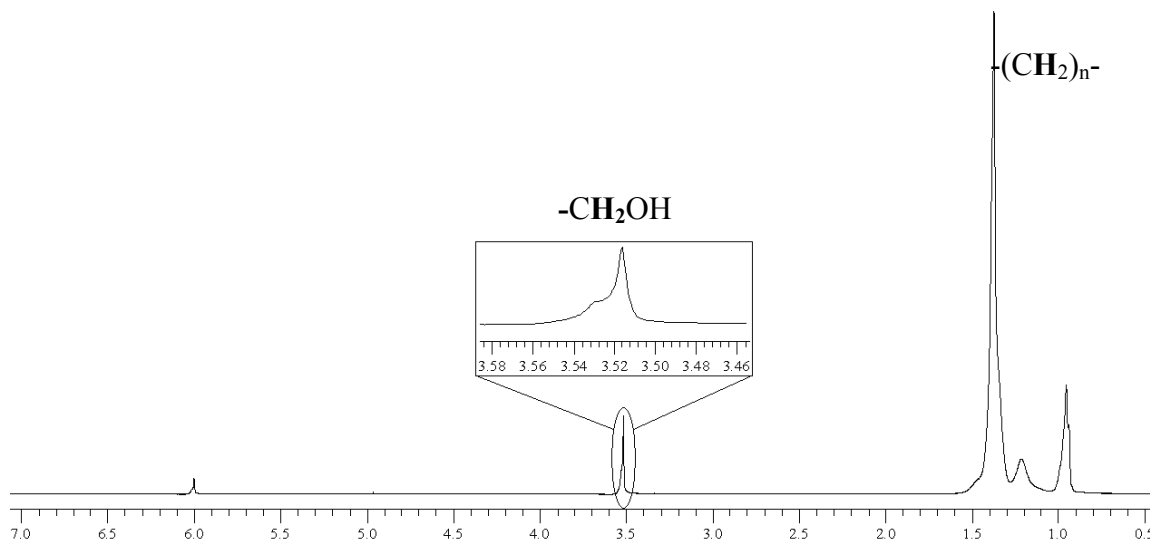
Figure 13-2: ^{1}H-NMR spectrum (Run 29, 9.8 mol %, 400 MHz, TCE-d$_2$, 120 ºC) of poly(ethylene-*co*-(but-3-enol))

The peaks at δ 3.52 or δ 3.54 are attributable to the α-protons of the incorporated monomer. The copolymers were analyzed by IR spectroscopy to confirm the incorporation of the polar monomer. Figures 13-3 and 13-4 show the IR spectra of the copolymers with 3.0 and 9.8 mol % incorporated but-3-enol respectively. The characteristic –OH stretch around 3400 cm^{-1} was distinct for the copolymer with 9.8 mol % incorporated but-3-enol (Run 29). The C-H stretches were also present at 2900-2850 cm^{-1} along with the C-H bending modes at 1470 and 1375 cm^{-1}. The C-O stretches were also observed at 1137 and 1131 cm^{-1} in Figures 13-3 and 13-4 respectively.[32]
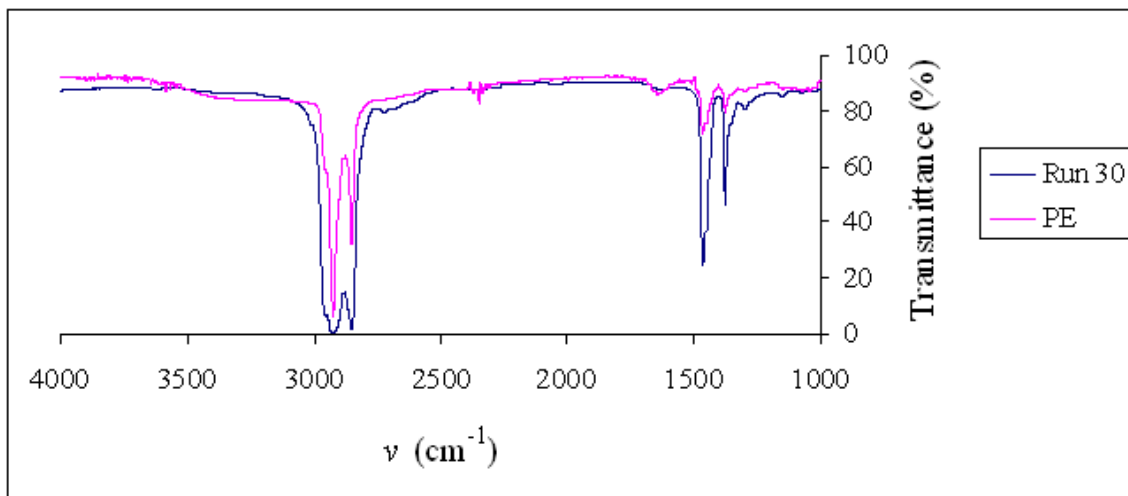
Figure 13-3: Transmittance infrared spectrum (film) of poly(ethylene-*co*-(but-3-enol)) (Run 30, 3.0 mol %)
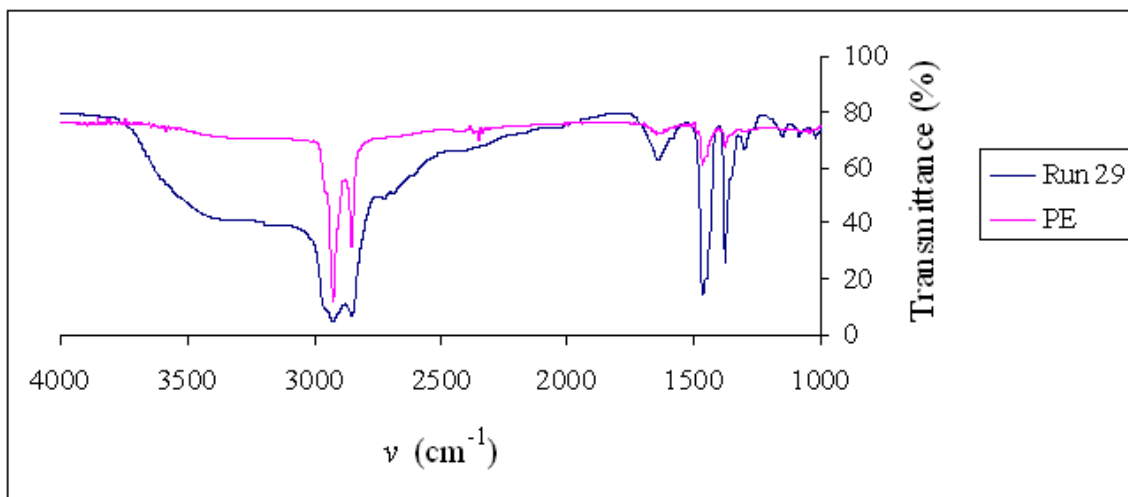
Figure 13-4: Transmittance infrared spectrum (film) of poly(ethylene-*co*-(but-3-enol)) (Run 29, 9.8 mol %)

Table 3: Copolymerization results of poly(ethylene-*co*-(but-3-enol)).[a]

Run	MAO (equiv.)	Moles of precatalyst (×10⁶)	Comonomer (equiv.)	Initial Temp. (ºC)	Yield (g)	Catalyst Activity (kg/mol)	Mol % incorp.[b]
25	1000	14	100	25	0.58	40	0.00
26	1000	15	100	25	1.1	70	0.07
27	1000	15	50	25	2.6	170	0.00
28	1000	14	50	0	2.3	160	0.69
29	1000	16	50	25	2.1	130	9.8
30	1000	16	50	60	0.69	40	3.0

[a] Copolymerizations were run for 30 min [b] Determined from ^{1}H-NMR spectra analyses using equation 3-6. [Ethylene] is 0.13 M and 0.08 M at 25 ºC and 60 ºC respectively.[30b]

The results in Table 3 show that there are no overall trends with these copolymerizations. There was a distinct lack of reproducibility of the results (Run 25 and Run 26). The highest incorporation reported was 9.8 mol % (Run 29). The percentage incorporation was determined using equation 3-6 where ACH_2O represented the integration of the α-protons (δ 3.52 or 3.54) from the but-3-enol alcohol incorporated into the polyethylene backbone. $ACH_{2(PE)}$ represented the integration of the methylene protons (δ 1.4) from the polyethylene backbone (4 from ethylene plus 4 from but-3-enol).

Mol % incorporation = $(ACH_2O/2) / [(ACH_{2(PE)})/2]$ **eq. 3-6[*]**

[*] Derivation of eq. 3-6 can be found in the appendix

Upon further analysis of the DSC traces of the poly(ethylene-*co*-(but-3-enol))

samples, no T_m were observed. This shows that the materials produced were not

crystalline. The results from these copolymerizations provide additional proof that more

work has to be done to understand why upon duplicating the reaction conditions (Run 27

and Run 29) different results are obtained. The catalyst activity seems to be unaffected by

changes in the initial temperature of the reaction (Run 25 and Run 30).

3.4.3 Copolymerization with (dec-9-enyloxy)trimethylsilane

All copolymers were analyzed by ^{1}H-NMR and IR spectroscopy and DSC analysis where possible. Figures 14-1, 14-2 and 14-3 show the ^{1}H-NMR spectra of poly(ethylene-*co*-(dec-9-enol)) with 0.97, 1.6 and 2.6 mol % incorporated dec-9-enol. The triplet at δ 3.70 is attributable to the α-protons of the incorporated monomer and the quintet at δ 1.65 is attributable to the β-protons. The absence of olefinic resonances between δ 5- 6 demonstrates the absence of unincorporated comonomer.
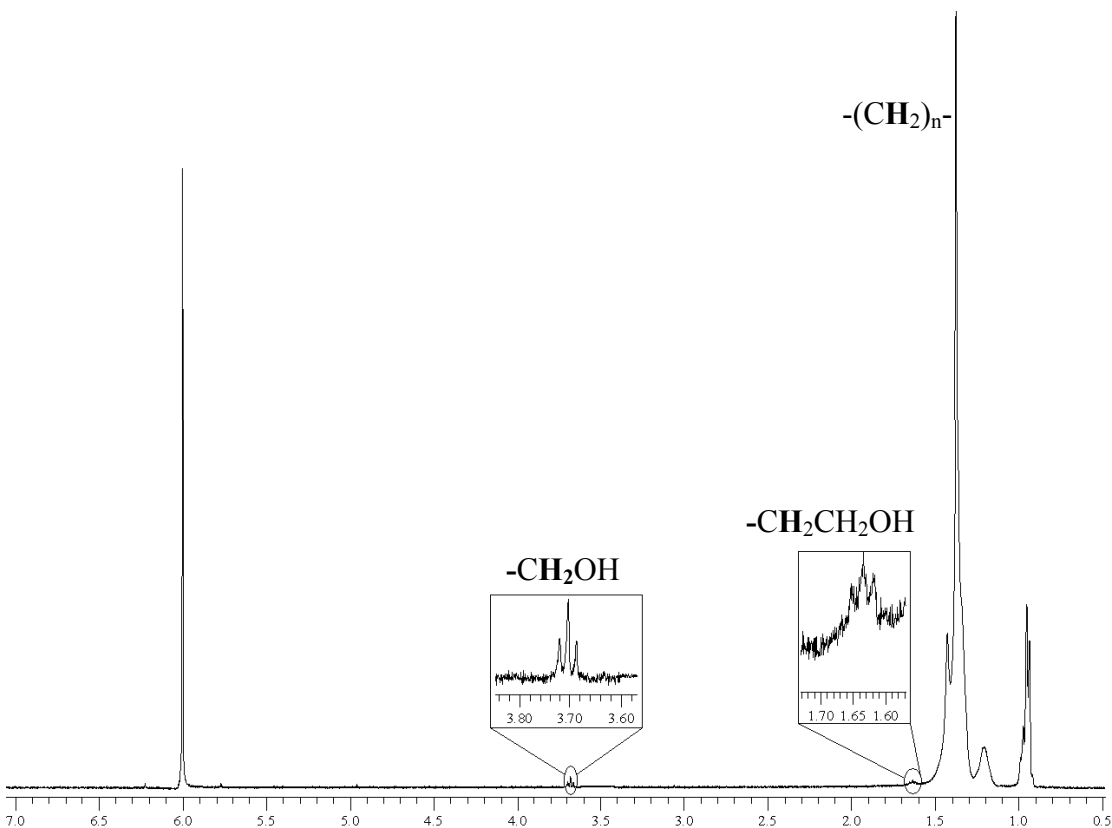
Figure 14-1: ^{1}H-NMR spectrum (Run 23, 0.97 mol %, 400 MHz, TCE-d$_2$, 120 ºC) of poly(ethylene-*co*-(dec-9-enol))
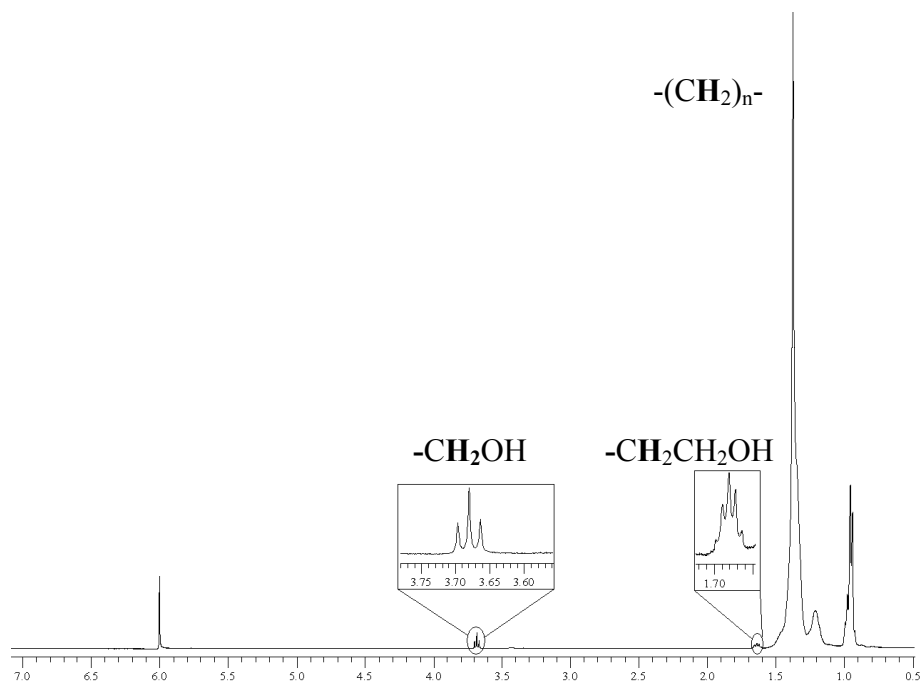
Figure 14-2: ^{1}H-NMR spectrum (Run 24, 1.6 mol %, 400 MHz, TCE-d$_{2}$, 120 ºC) of poly(ethylene-*co*-(dec-9-enol))
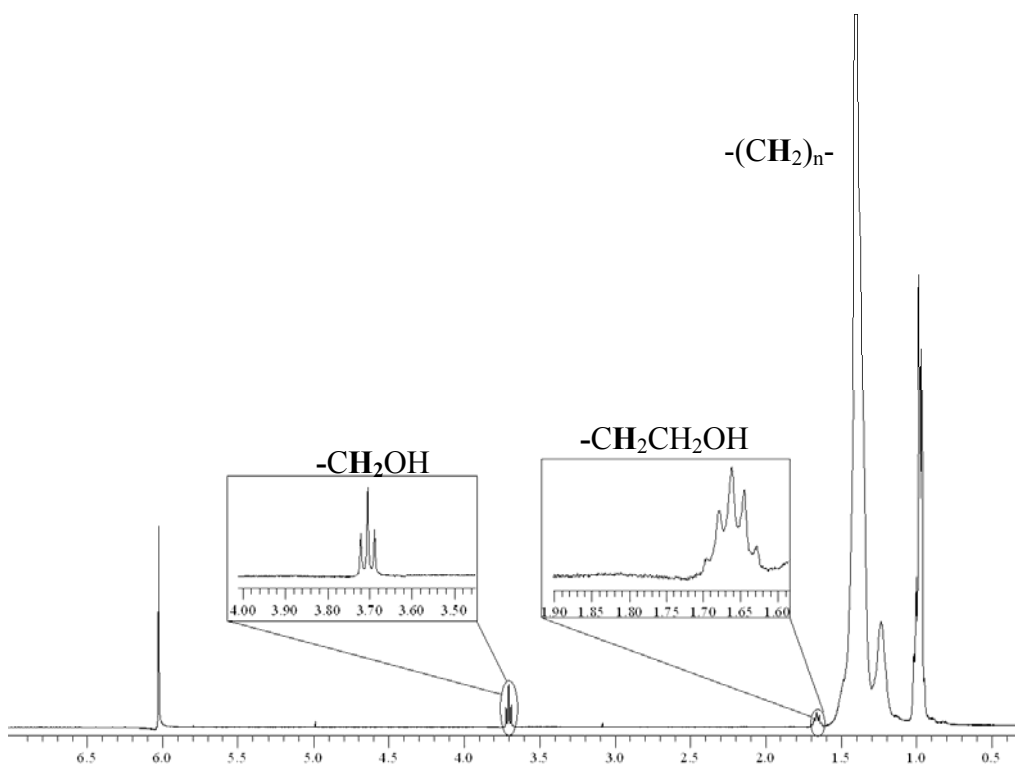
Figure 14-3: ^{1}H-NMR spectrum (Run 20, 2.6 mol %, 400 MHz, TCE-d$_{2}$, 120 ºC) of poly(ethylene-*co*-(dec-9-enol))

The copolymers were analyzed by IR spectroscopy to confirm the incorporation of the polar monomer. Figures 14-4, 14-5 and 14-6 show the IR spectra of poly(ethylene-*co*-(dec-9-enol)) with 0.97, 1.6 and 2.6 mol % incorporation respectively. The characteristic –OH stretch around 3400 cm^{-1} was present. The stretch was sharper than those observed with the other two comonomers. This is consistent with less hydrogen bonding within the solid polymer because of the longer dec-9-enol side chains. The C-H stretches were also present at 2900-2850 cm^{-1} along with the C-H bending modes at 1470 and 1375 cm^{-1}. C-O stretches at (1050 and 1143 cm^{-1}), (1041 and 1115 cm^{-1}) and 1041 cm^{-1} were also observed in Figures 14-4, 14-5 and 14-6 respectively.[32]
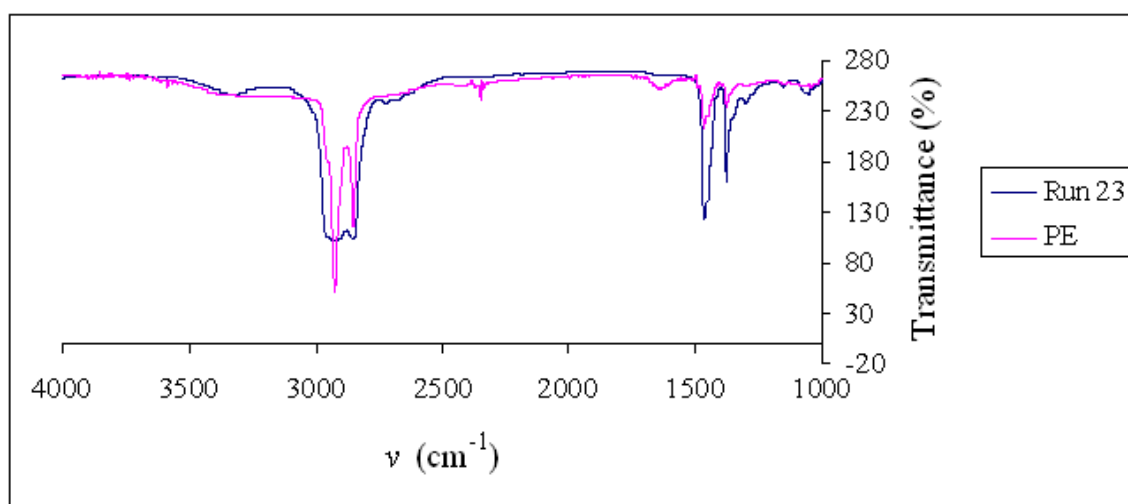
Figure 14-4: Transmittance infrared spectrum (film) of poly(ethylene-*co*-(dec-9-enol)) (Run 23, 0.97 mol %)
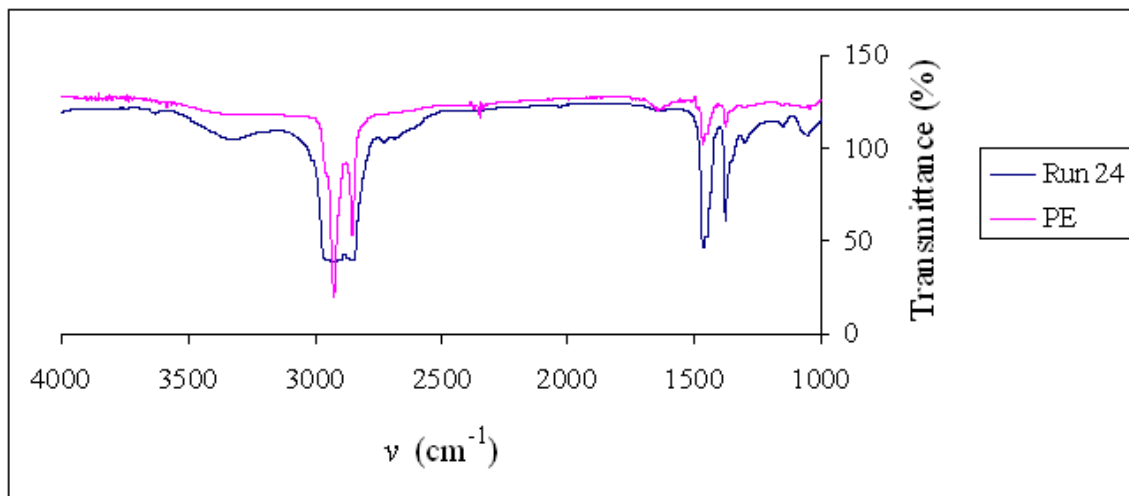
Figure 14-5: Transmittance infrared spectrum (film) of poly(ethylene-*co*-(dec-9-enol)) (Run 24, 1.6 mol %)
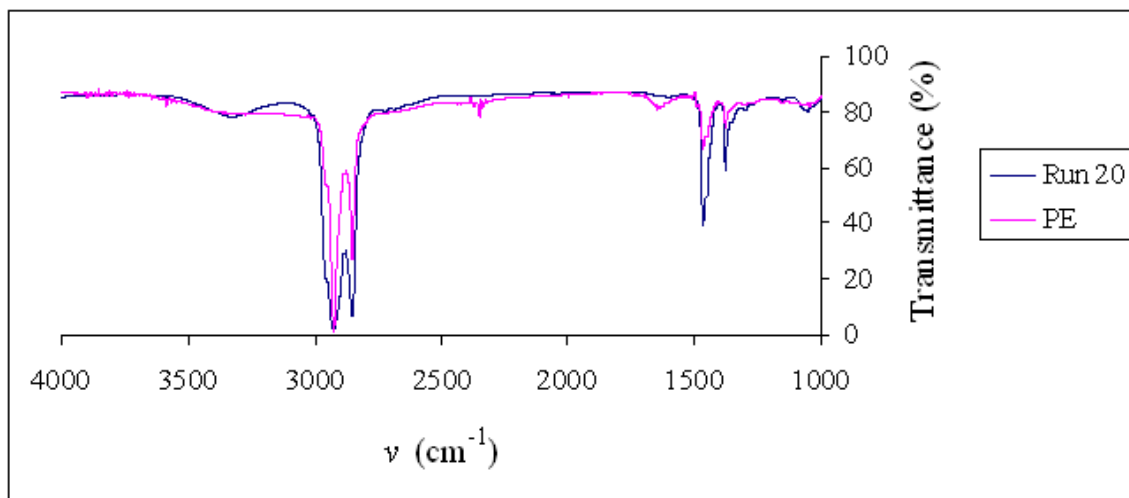
Figure 14-6: Transmittance infrared spectrum (film) of poly(ethylene-*co*-(dec-9-enol)) (Run 20, 2.6 mol %)

63

Table 4: Copolymerization results of poly(ethylene-*co*-(dec-9-enol)).[a]

Run	MAO (equiv.)	Moles of precatalyst (×10^6)	Comonomer (equiv.)	Initial Temp. (°C)	Yield (g)	Catalyst Activity (kg/mol)	Mol % incorp.[b]
19	1000	16	100	25	0.60	40	0.00
20	1000	15	100	25	1.6	100	2.6
21	1000	18	50	25	1.7	90	1.3
22	1000	15	50	0	0.96	60	1.9
23	1000	15	50	25	1.8	120	0.97
24	1000	15	50	60	0.75	50	1.6

[a] Copolymerizations were run for 30 min [b] Determined from ^{1}H-NMR spectra analyses using equation 3-7. [Ethylene] is 0.13 M and 0.08 M at 25 °C and 60 °C respectively.[30b]

Table 4 shows that there was an overall lack of reproducibility. Previous researchers had found that higher degrees of incorporation were obtained with polar monomers which had longer spacer (methylene) groups (C_6 and higher) between the polar functionality (-OH) and the C=C double bond.[33] This, however, was not observed with this system. The highest incorporation reported was 2.6 mol % (Run 20). The percentage incorporation was determined using equation 3-7 where ACH_2O represented the integration of the α-protons (δ 3.70) from the dec-9-enol alcohol incorporated into the polyethylene backbone. $ACH_{2(PE)}$ represented the integration of the methylene protons (δ 1.4) from the polyethylene backbone (4 from ethylene and 7 from dec-9-enol).

Mol % incorporation = $(ACH_2O/2)$ / $[(ACH_{2(PE)})/4 - (3ACH_2O)/8]$ **eq. 3-7**[*]

[*] **Derivation of eq. 3-7 can be found in the appendix**

From the DSC traces of poly(ethylene-*co*-(dec-9-enol)), no distinct T_m were found. This is consistent with a material that is not crystalline. This is mainly due to the incorporation of dec-9-enol in combination with long branches along the polymer main chain.

Overall the activity of the catalyst was unaffected by varying the initial reaction temperature (Run 19 and Run 24). With this catalytic system, the length of the spacer group is not as important to achieve higher degrees of incorporation. These materials may have interesting applications in the future.

3.5.0 Conclusions

In this thesis the results of an investigation of the copolymerization of ethylene with $CH_2=CH(CH_2)_nOSiMe_3$ (n = 1, 2, 8) were presented. The desired copolymers having polar $-(CH_2)_nOH$ branches were obtained by acid catalyzed hydrolysis using acidified methanol.

Percentage incorporations of up to 9.0 mol % were reported with the (allyloxy)trimethylsilane comonomer. The IR spectra of the copolymers showed the characteristic –OH stretch at 3400 cm^{-1}. The absence of distinct T_m in the DSC traces demonstrated that the materials produced were not crystalline.

The highest percentage incorporation obtained from the poly(ethylene-*co*-(but-3-enol)) copolymerizations was 9.8 mol %. On the other hand, with (dec-9-enyloxy)trimethylsilane, up to 2.6 mol % incorporation was obtained.

This shows that with this catalytic system, the length of the spacer group is not important to achieve higher degrees of incorporation.

Overall, with all three comonomers, there was a lack of reproducibility of the results. This was observed from the analysis of the materials produced from reactions were the reaction conditions were duplicated. There were no direct correlations with the activity of the catalyst and the reaction conditions (catalyst loading, reaction temperature).

Based on the results obtained with this project, future work in this area will involve the use of different diimine ligands around the nickel centre. This will investigate whether or not the ligand structure is instrumental to comonomer incorporation. This project provided evidence that there are still unknown variables which affect the

incorporation of polar functionalities into polyolefins. The materials produced may have

interesting applications in the future.

References

[1] Schrekker, H.S.; Kotov, V.; Preishuber-Pflugl, P.; White, P.; Brookhart, M. *Macromolecules*, **2006**, 39, 6341

[2] Balsam, M.; Baum, P.; Engelmann, J. *Macromol. Mater. Eng.*, **2001**, 286(4), A7

[3] Peacock, A. J. *Polym. Mater. Sci. Eng.,* **1999**, 80, 291

[4] (a) Peacock, A. J. *Handbook of Polyethylene: Structure, Properties, and Applications*; Marcel Dekker: New York, **2000**, (b) Stevens, M. P. *Polymer Chemistry: An Introduction*; Oxford University Press, New York, **1999**, (c) Shultz, L. H.; Brookhart, M. *Organometallics*, **2001**, 20 (19), 3975

[5] Kaminsky, W.; Laban, A. *Appl. Catal., A.,* **2001**, 222, 47

[6] Witcoff, H. A.; Reuben, B. G.; Plotkin, J. S. *Industrial Organic Chemicals;* John Wiley & Sons: New York, **2004**

[7] Ittel, S.; Johnson, L.; Brookhart, M. *Chem. Rev.,* **2000**, 100, 1169

[8] Ziegler, K. *Angew. Chem.,* **1964**, 76, 545

[9] Natta, G. *Science,* **1965**, 147, 261

[10] (a) Brintzinger, H. H.; Fischer, D.; Mülhaupt, R.; Rieger, B.; Waymouth, R. *Angew. Chem.* **1995**, 107, 1255, (b) *Angew. Chem., Int. Ed. Engl.* **1995**, 34, 1143

[11] Yanjara, M. J.; Sivaram, S. *Prog. Poly. Sci.* **2002**, 27, 1347

[12] Chung, T. C. *Macromolecules,* **1988**, 21, 865

[13] Sivak, A. J.; Cullo, L. A. Ziegler-Natta polymerization of siloxy group containing alkenes in preparation of polymers containing functional groups. PCT Int. Appl. **1988,** 59 pp. CODEN: PIXXD2 WO 8808856 A1 19881117; U. S. Patent 8703454; Aristech Chemical Corporation

[14] Pritchard, J. G. *Polyvinyl Alcohol, Basic Properties and Uses;* Gordon and Breach: New York, **1971**

[15] Ramakrishnan, S.; Berluche, E.; Chung, T. C. *Macromolecules*, **1990,** 23, 378

[16] Lu, H. L.; Chung, T. C. *Journal of Molecular Catalysis A: Chemical,* **1997**, 115, 115

[17] Breslow, D. S.; Newburg, N. R. *J. Am. Chem. Soc.* **1957**, 79, 5072

[18] Sinclair, K. B.; Wilson, R. B. *Chem. Ind.* **1994**, 21, 857

[19] Aulbach, M.; Küber, F. *Chem. Unserer Zeit* **1994**, 26, 197

[20] Brintzinger, H. H.; Fischer, D.; Mülhaupt, R.; Rieger, B.; Waymouth, R. *Angew Chem.* **1995**, 107, 1255, *Angew. Chem., Int. Ed. Engl.* **1995**, 34, 1143

[21] Kaminsky, W.; Arndt, M. *Adv. Polym. Sci.* **1997**, 127, 143

[22] Alt, H. G. *Russ. Bull.* **1995**, 44, 1

[23] Du Mont, W. W.; Weidenbruch, M.; Grochman, A.; Bochmann, M. *Nachr. Chem. Tech. Lab.* **1995**, 43, 115

[24] (a) Sinn, H.; Kaminsky, W. *Adv. Organomet. Chem.* **1980**, 18, 99, (b) Earley, C. W. *Journal of Molecular Structure: THEOCHEM*, **2007**, 805, 101, (c) Atwood, J. L.; Hrneir, D. C.; Priester, R. D.; Rogers, R. D. *Organometallics*, **1983**, 2, 985

[25] Ewen, J. A.; Jones, R. L.; Razavi, A.; Ferrara, J. D**.** *J. Am. Chem. Soc.* **1988**, 110, 6255

[26] (a) Johnson, L. K.; Killian, C. K.; Brookhart, M. *J. Am. Chem. Soc.,* **1995**, 117, 6414 (b) Bertini, I.; Luchinat, C.; Parigi, G. *Solution NMR of Paramagnetic Molecules-Applications to Metallobiomolecules and Models.* Elsevier Science, **2001**, Chap. 5, 187 (c) Han, C. J; Lee, M. S.; Byun, D.; Kim, S. Y. *Macromolecules*, **2002**, 35, 8923, (d) Kaneyoshi, H.; Matyjaszewski, K. *Journal of Applied Polymer Science*, **2007**, 105, 3

[27] Samuel, E.; Rausch, M. D. *J. Am. Chem. Soc.* **1973**, 95, 6263

[28] Paulovicova, A.; El-Ayaan, U.; Shibayama, K.; Morita, T.; Fukuda, Y. *Eur. J. Inorg. Chem.* **2001**, 2641

[29] Ward, L. G. L. *Inorganic Synthesis,* **1972**, 13, 154

[30] (a) Azizi, N.; Saidi, M. R. *Organometallics*, **2004**, 23, 1457, (b) McKnight. A. L.; Waymouth, R. M. *Macromolecules,* **1999**, 32, 2816, (c) Braun, F.; Willner, L.; Hess, M.; Kosfeld, R. *Journal of Organometallic Chemistry*, **1987**, 332, 63

[31] (a) Azizi, N.; Saidi, M. R.; Yousefi, R. *J. Organometallic Chem,* **2006**, 691, 817, (b) Yakelis, N.A; Bergman, R. G. *Organometallics*, **2005**, 24 (14), 3579, (c) Fox, H. H; Schrock, R. R. *Organometallics*, **1994**, 13, 635

[32] Silverstein, R. M.; Webster, F. X. *Spectrometric Identification of Organic Compounds*, 6th ed.; John Wiley and Sons: New York, **1998**, 83

[33] (a) Kimmo, H., Löfgren, B., Helaja, T. *Eur. Polym. J.* **1998**, 34, 1093

(b) Goretzki, R., Fink, G. *Macromol. Rapid. Commun.* **1998**, 19, 511

[34] (a) Kashiwa, N., Imuta, J., Toda, Y. *J. Am. Chem. Soc.* **2002**, 124, 1176

(b) Kashiwa, N., Matsugi, T., Imuta, J. *J. Polym. Sci: Part A: Polymer Chemistry,* **2003**, 41, 3657

Appendix

Derivation of equations used to calculate percentage incorporation (mol %)

Poly(ethylene-*co*-allyl alcohol)

$ACH_2O = 2 * allyl\ alcohol$　　　　　　　　　**(1)**

$ACH_{2(PE)} = 4 * ethylene + 2 * allyl\ alcohol$

$ethylene = [ACH_{2(PE)} - 2 * allyl\ alcohol] / 4$

Therefore, $ethylene = [ACH_{2(PE)} - ACH_2O] / 4$　　　　**(2)**

Mol % incorporation = allyl alcohol / [ethylene + allyl alcohol]

Mol % incorporation $= (ACH_2O/2) / [(ACH_{2(PE)} - ACH_2O)/4 + ACH_2O/2]$　　　**eq. 3-5**

ACH_2O represents the integration of the α-protons (δ 3.52) from the allyl alcohol incorporated into the polyethylene backbone. $ACH_{2(PE)}$ represents the integration of the methylene protons (δ 1.4) from the polyethylene backbone.

Poly(ethylene-*co*-(but-3-enol))

$ACH_2O = 2 * but\text{-}3\text{-}enol$　　　　　　　　　**(1)**

$ACH_{2(PE)} = 4 * ethylene + 4 * but\text{-}3\text{-}enol$

$ethylene = [ACH_{2(PE)} - 4 * but\text{-}3\text{-}enol] / 4$

Therefore, $ethylene = [ACH_{2(PE)} - 2(ACH_2O)] / 4$　　　　**(2)**

Mol % incorporation = but-3-enol / [ethylene + but-3-enol]

Mol % incorporation $= (ACH_2O/2) / [(ACH_{2(PE)} - 2(ACH_2O))/4 + ACH_2O/2]$

Mol % incorporation $= (ACH_2O/2) / [(ACH_{2(PE)})/2]$　　　　　**eq. 3-6**

ACH_2O represents the integration of the α-protons (δ 3.52 or 3.54) from the but-3-enol alcohol incorporated into the polyethylene backbone. $ACH_{2(PE)}$ represents the integration of the methylene protons (δ 1.4) from the polyethylene backbone.

Poly(ethylene-*co*-(dec-9-enol))

$ACH_2O = 2 * dec\text{-}9\text{-}enol$ **(1)**

$ACH_{2(PE)} = 4 * ethylene + 7 * dec\text{-}9\text{-}enol$

ethylene = $[ACH_{2(PE)}\ -\ 7 * dec\text{-}9\text{-}enol]\ /\ 4$

Therefore, ethylene = $[ACH_{2(PE)} - 7/2(ACH_2O)]\ /\ 4$ **(2)**

Mol % incorporation = dec-9-enol / [ethylene + dec-9-enol]

Mol % incorporation = $(ACH_2O/2)\ /\ [(ACH_{2(PE)})/4 - 7(ACH_2O)/8 + (ACH_2O)/2]$

Mol % incorporation = $(ACH_2O/2)\ /\ [(ACH_{2(PE)})/4 - (3ACH_2O)/8]$ **eq. 3-7**

ACH_2O represents the integration of the α-protons (δ 3.70) from the dec-9-enol alcohol incorporated into the polyethylene backbone. $ACH_{2(PE)}$ represented the integration of the methylene protons (δ 1.4) from the polyethylene backbone.